Induction of defense responses in tobacco by harpin biofunctionalized nanoparticles

Thesis submitted to the University of Hyderabad for the award of Doctor of Philosophy

By

Sippi Issac Kongala

(Regd. No: 05LPPH10)

Department of Plant Sciences
School of Life Sciences
University of Hyderabad
Hyderabad – 500046 India

June, 2017

University of Hyderabad

(A Central University established in 1974 by act of parliament)

HYDERABAD – 500 046, INDIA

DECLARATION

I **Sippi Issac Kongala,** hereby declare that this thesis entitled ***"Induction of defense responses in tobacco by harpin biofunctionalized nanoparticles"*** submitted by me under the guidance and supervision of **Prof. Appa Rao Podile** an original and independent research work. I also declare that it has not been submitted previously in part or in full to this University or any other University or Institution for the award of any degree or diploma. A report on plagiarism statistics from University Librarian is enclosed.

Sippi Issac Kongala
(05LPPH10)

Prof. Appa Rao Podile
(Research Supervisor)

University of Hyderabad

(A Central University established in 1974 by act of parliament)

HYDERABAD – 500 046, INDIA

CERTIFICATE

This is to certify that this thesis entitled **"Induction of defense responses in tobacco by harpin biofunctionalized nanoparticles"** is a record of bonafide work done by **Mr. Sippi Issac Kongala** a research scholar for Ph.D. programme in Department of Plant Sciences, School of Life Sciences, University of Hyderabad under my guidance and supervision.

Prof. Appa Rao Podile
(Research Supervisor)

Head,
Department of Plant Sciences

Dean,
School of Life Sciences

CONTENTS

Acknowledgements

This Report would not have been possible without the essential and gracious support of many individuals.

I take immense pleasure in thanking Prof. Appa Rao Podile, Head, MPMI Group, who had been a source of inspiration and role model in any given way, for his constant moral and personal support and guidance throughout my doctoral research. The leadership and critical assessment capabilities of Prof. Podile, allowed me to mobilize my collective knowledge and capacity in the best way possible and created an enabling environment to complete my research work.

I thank the present and former Deans, School of Life Sciences, Prof. P.Reddanna and Prof. A. S. Raghavendra, the present and former Heads, Department of Plant Sciences Prof. CH.Venkata Ramana and Prof. P. B. Kirti for allowing me to use the facilities of the School and the Department. I sincerely acknowledge the infrastructural support provided by UGC, DST-Centre for Nanotechnology, to the Dept.of Plant Sciences and Govt of India for the research fellowship.
.
This thesis is not only the result of my scientific works but the outcome of a long road and I am glad to acknowledge everyone who has contributed to the build-up of my scientific personality and therefore, to the completion of this thesis.

Here again I thank my supervisor Prof. Podile and late Mrs. Padmaja Podile for their love, care and affection, which made me to forget my home.

My heartfelt thanks are also due to my former colleague scholars of MPMI group Dr. M. Praveen, B. Sashidhar, Dr. Ch. Neeraja, Dr. V.

L. Vasudev, and Dr. Aravind, Dr. Debashish for their timely help and constant encouragement.

I would like now to mention “some” of my colleagues who have made the last few years so cheerful. Dr. Sharma, Papa Rao, Deb, Suma, Purushotham, Uma, Swaroopa, Suprava, Das, Manjeet, Madhu, Parvati, Srinu, Raju, Satyavathi, Rambabu, Ritika, Sravani and who’ve been very cooperative in more ways than one.

This dissertation work at MPMI group could never run smoothly without all the help I got from all technicians. I wish to thank my lab technicians Narasimha, Malla Reddy and Devaiah for their assistance in the lab and in the green house.

I am thankful to all my batch mates and other research scholars of the School of Life Sciences for their timely help of Ramesh, Mohan Rao and Sudarshanam and other non-teaching staff is acknowledged.

I express very special and heartfelt thank for their timely help and highly acknowledge the efforts of Dr. M. Praveen, Sarma PVSRN, and Papa Rao V.

Saving the most important for the last, I would like to express my heartfelt thanks to my beloved wife K. Surekha and my parents K. Jonah and Nalinakshi Joseph for their blessings, wishes, support and constant encouragement throughout my research carrier.

K. SIPPI ISSAC

Dedicated to...

my mentor Prof. A.R. Podile
and my family

ABBREVIATIONS

µg : microgram

µM : micromolar

°C : degree centigrade/degree Celsius

AFM: Atomic Force Microscopy

Abs : absorption

Bp : base pair

BSA : bovine serum albumin

cDNA : complementary

CTAB: Cetyl trimethyl ammonium bromide

DEPC : diethylpyrocarbonate

DMSO : dimethyl sulfoxide

DNA : deoxy ribonucleic acid

dNTPs : deoxy nucleotide triphosphates

Ea : *Erwinia amylovora*

EDTA : ethylene diamine tetra acetic acid

EDAX: energy dispersive xray spectroscopy

g : gram

h : hour(s)

HR : hypersensitive response

Hrp : hypersensitive response pathogenicity

hrpZ : gene encoding harpin

IPTG : isopropyl β-D-thiogalactoside

ISR : induced systemic resistance

kb : kilobase pair

kDa : kilodalton

L : litre

LB : Luria-Bertani

LS : leader sequence

M : molar

mg : milligram

min : minute

ml : milliliter

mM : millimolar

NBT : nitroblue tetrozolium

Ni-NTA : nickel-nitroacetic acid agarose

nm : nanometers

OD : optical density

ORF : open reading frame

PAGE : polyacrylamide gel electrophoresis

PBS : phosphate buffered saline

PCD : Programmed cell death

PCR : polymerase chain reaction

PMSF : phenylmethylsulfonylfluoride

PR proteins : pathogenesis-related proteins

Pss : *Pseudomonas syringae* pv. *syringae*

Pst : *Pseudomonas syringae* pv. *tomato*

RNA : ribonucleic acid

RNase : ribonuclease

ROS : reactive oxygen species

rpm : revolutions per minute

RT-PCR : reverse transcriptase-polymerase chain reaction

SAR : systemic acquired resistance

SDS : sodium dodecyl sulphate

sec : seconds

SEM : scanning electron microscopy

SP : signal peptide

TE : Tris-EDTA

TEM: transmission electron microscopy

TMV : tobacco mosaic virus

Tris : tris-(Hydroxymethyl) aminoethane

TTSS : type three secretion system

UV-VIS: UV Visible spectrophotometry

V : volts

X-gal : 5-bromo-4-chloro-3-indolyl β-D- galactoside

List of figures:

List of tables:

Introduction

1. REVIEW OF LITERATURE

1.1 Nanotechnology

Nanotechnology has become a buzz word of 21st century due to its immense applications for human kind. Nanotechnology is defined as technology dealing with Nano-sized particles wherein Nano meaning dwarf which is derived from Greek. The word Nano refers to one billionths of a meter or 10^{-9} meter as shown in the Figure 1.1. Nanotechnology involves manipulation at the atomic or molecular scale to transform biosystems USEPA (2007). Due to formation of Nano sized particles, these tiny particles attain novel properties affecting their size (solubility, transparency, colour, absorption, conductivity, etc) and surface (dispersibility, catalytic behaviour, optical properties, etc) offering innumerable opportunities and exhaustively explored for betterment of mankind.

Currently, Nanotechnology has revolutionized the applications in the field of medicine, pharmacy, engineering, agriculture and other allied sciences (Singh HB et al. 2017). The Nano scale science coupled with above mentioned allied sciences has brought several opportunities and now entered a commercial era (Mazzola 2003; Paull et al. 2003). Some of the important applications of Nanotechnology in medicine include; enzyme labelling using fluorescent materials (Bruchez et al. 1998: Wang S et al. 2002) efficient delivery of drugs on to the target site (Mah et al. 2000: Panatarotto et al. 2003) detection of harmful microorganisms (Edelstein et al. 2000) treating several cancer related diseases (Yoshida et al. 1999) etc. Particularly, the integration of Nanotechnology with medicine resulted in huge explorations wherein several diagnostic and therapeutic tools are now available

in the market for better, imaging, sensing, and artificial implantation (Waren and Nie. 1998 : Vaseashta and Malinovska, 2005 : Sachlos et al. 2006). Nanotechnology has taken a lead in food industry with several applications including, smart packaging, improved preservatives, enhanced flavour/colours and added nutritional elements (Nasongkla et al. 2006).

1.2.Nanotechnology to measure and understand biosystems

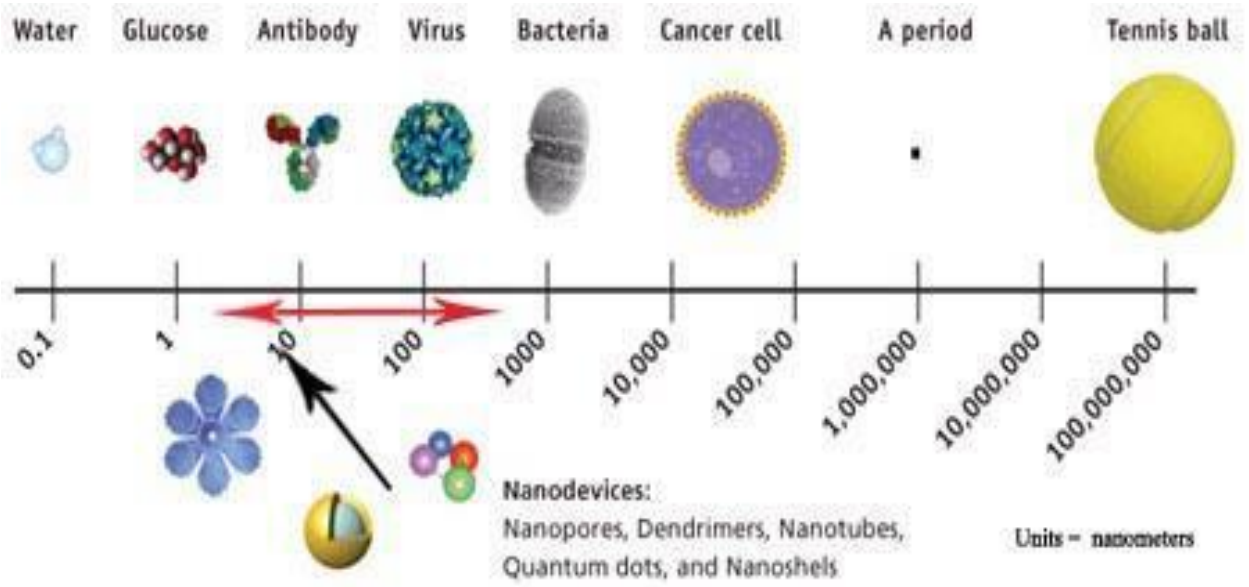

Figure 1.1: Schematic representation of Nanoscale particles. The depicted scale represents various sizes of materials observed in daily life (source: Randy Apple Gate – Centre for Diversity in Engineering).

The advances in Nanotechnology have facilitated biological scientists for easy quantification of cellular products revealing the molecular intricacies of cell such as self-repairing and self-replicating mechanisms. It enables single molecule measurements and to study the dynamics mechanistic properties of molecular biomachines. It also allows direct study of molecular motors, protein dynamics, enzyme reactions, DNA transcription and cell signalling. The measurement of chemical composition within a cell *in vivo* is now possible due to the

technical advances made with Nanotechnology. The Atomic force microscopy enables us to understand Intra and inter molecular mechanics of proteins, polypeptides, polymer molecule and Nanoparticles (Ikai et al. 2002). The Nanoscale technology output has opened doors to quantify Nano RNA'S (RNA ranging in length between 21 and 28 nucleotides) and their prominent effect on gene expression (Couzin 2002).

One of the prominent advances in application of Nanotechnology with microbial systems is deciphering interfacial and adhesive forces between living bacteria and mineral surfaces (Lower et al. 2001). Nanotechnology has brought a breakthrough in protein biochemistry with easier understanding of protein and folding and unfolding studies and further visualization of structural changes of proteins in living systems is also possible with the Nanotools (Baneyx et al. 2001). The measurement of intracellular forces, special and temporal interaction among cells can be done by Nanotechnology. Atomic Force Microscopy can be used to measure the binding strength between a single pair of molecules in physiological solutions (Misevic 2001). Also, Chemo-mechanical energy conversions related to intracellular processes and the motion of kinesin along microtubules explained with the above mentioned technology (Fox et al. 2001). Quantum dots have been developed for imaging and elected as markers for biological processes. The slower photo bleach of quantum dots and their finely tuned emission wavelength has advantage over fluorescent dye molecules (Dubertret et al.1999). Measurements of interneuronal synapse circuits and diameter of synaptic vesicles can be made by the advancement of Nanotechnology. The investigative tools of Nanotechnology utilized to study self-organization, assembly dynamics and supramolecular chemistry (Davis et al.2002).

1.3.Nanoparticles in plant growth

The Nano-sized materials are effectively used in plant germination and growth. The multiwalled carbon Nanotubes has greatly influenced the growth in tobacco cultures by 55% by regulating seed germination and plant growth (Khodakovskaya et al. 2012). The carbon Nanotubes influenced the expression of aquaporin NtPIP1, CycB and NtLRX1 which are involved in cell division or cell wall formation and water transport. The accumulation of Nanomaterials plays a prominent role in enhancing seed germination rate. The carbon Nanotubes activates the water channel (aquaporins) and gene regulators of cell division and extension. The use of multiwalled carbon Nanotubes increased in the germination rate by 90% in tomato (Khodakovskaya et al. 2009). Carbon Nanotubes can breach the tough coat of tomato seeds and enhances the growth due to water upregulation without in any severe effects on the plant growth.

The influence of nano and non-nano TiO2 on the germination of spinach seeds were observed by Zheng et al. 2005. Observations indicated that 73% upregulation of chlorophyll formation and the photosynthetic rate was increased by thrice in comparison with control. The superoxide and hydroxide anions causes photo sterilization and photogeneration by treating with Nano TiO_2 which play an important role in seed germination and growth of spinach seeds. Resistance to pests also observed which were germinated through carbon Nanotubes. Germination is effected by the size of Nanoparticles. As the particle size decreases, it increases the germination of growth. Canola seeds treated with Nano-sized titanium dioxide increased seed vigour with that of control (Mahmoodzadeh et al. 2013). 1000 ppm concentration of Zinc oxide Nanoparticles increased the seed germination (Prasad et al. 2012). It also exhibited onset of flowering, higher chlorophyll leaf content, also enhanced stem and root growth in plants.

1.4 Nanotechnology in plant pathogen control

The bacterial agents which are more commonly affect the vegetables are *Erwinia carotovora, Corynebacterium, Pseudomonas spp* and *Xanthomonas campestris.* The spoilage of vegetables by fungal pathogens include species belonging to genera *Cladosporium, Colletotrichum, Phomopsis, Alternaria, Aspergillus, Pythium, Phytophthora, Fusarium, Penicillium, Phoma, , Rhizopus* spp*, Rhizoctonia solani, Botrytis cinerea, Sclerotinia sclerotiorum* and some powery and downy mildews. These microorganisms enter the plant through mechanical barriers and wounds. Most of the above mentioned microorganisms are host specific and cause a great damage to crops and some of them produce toxic compounds which badly affect humans. Till date, the toxicology of bactericides and fungicides (potentially involved in removing bacteria and fungi) revealed very less percentage (0.1%) of toxic effect on target organisms. Due to which, farmers has to invest heavily on large usage of bactericides and/or fungicides.

Nanomaterials have potential applications in crop protection as they have unique property of controlled release of loaded pesticide, fertilizer and other agrochemicals. The application of Nanosilver on cabbage black rot has shown a huge impact on successful removal of *Xanthomonas campaestris pv campestris* (Gan et al. 2010). The Validamyc loaded on to calcium carbonate showed improved resistance (post infestation of 7-days) towards *Rhizoctonia solani* compared with individual Validamycin treatment (Qian et al. 2011). Thiamine di-lauryl sulphate Nanoparticles at 100 ppm concentration showed inhibition of 80% growth in *Colletotrichum.gloeosporioides* compared to control. Chitosan Nanoparticles (6% w/v) delayed mycelia growth of *Colletotrichum capsici , Rhizopus sp., C. gloeosporioides and Aspergillus niger* with that of control (Chookhongkha et al. 2012*).* Nano copper decreased the growth of *Xanthomonas axonopodis* at a concentration range of 0.2 ppm (Mondal and Mani 2012).

1.5. Nanoparticles in crop protection.

1.5.1.Silver Nanoparticles

From ancient times silver nanoparticles are routinely used as antimicrobial agents due to their broad spectrum over several pathogenic strains (Jo et al 2009: Navin Jain et al 2010*).* It shows higher toxicity to microorganisms and with little to no toxicity on mammalian cells. Further, the preparation of silver nanoparticles is cheaper (Clement and Jarrett 1994). Due to environmental hazards and residual problem of pesticides, usage of silver as antimicrobial agent has enormously increasing. Nanosilver itself is identified as pesticide besides its role as plant- growth stimulator, inhibits unwanted microorganisms in soils (Baier 2009 : Sharma et al. 2012). The antifungal activity of colloidal Nano silver solution against rose powdery mildew was studied. The application of silver in inhibiting various plant pathogensis is a safer method compared to artificial fungicides (Park *et al. 2006).* Topical application of silver nanoparticles at 100 ppm concentration involved with pepper anthracnose against six *Colletotrichum* species effected the growth of fungal hyphae and conidial germination (Lamsal et al. 2011*).* Dose dependent fungistatic activity on *Colletotrichum gloesporioides* were studied by (Aguilar-Mendez et al. 2011). The antifungal activity of *Bipolaris sorokiniana* and *Magnaporthe grisea* revealed that they influence disease progress and colony formation of fungal spores (Jo et al. 2009). Silver nanoparticles showed drastic damage and resulted in the separation of hyphal wall layers and the deformation of fungal hyphae of sclerotium forming species *Rhizoctonia solani* and *Sclerotinia sclerotiorum* (Min et al. 2009). Maximum inhibition of fungal hyphae and conidial germination was observed in case of cucumbers and pumpkins against powdery mildew under *in vitro* and *in vivo* conditions *(*Lamsal et al. 2011b)**.**

1.5.2.Silica Nanoparticles

Application of silica Nanoparticles showed better antimicrobial activity in plants. The disease resistance and stress resistance were increased by silica Nanoparticles (Brecht et al. 2004). Physiological activity and growth of the plants was greatly influenced by silica Nanoparticles (Carver et al. 1998). Application of silica Nanoparticles was showed to be target specific movement of proteins, nucleotiodes and chemicals (Torney et al. 2007).

1.5.3.Copper Nanoparticles

Copper based Nanoparticles play an important role in disease occurence and involved in the treatment of variety of plants as they produce highly active hydroxyl radicals which disrupt proteins, lipids, DNA and biomolecules (Borkow and Gabbay 2005). *Fusarium graminearum* is inhibited by the chitosan Nanogels and copper by synergistic effect. As they possess bio-compatible nature these were employed as a new generation of copper- based bio-pesticides potentially involved in crop protection (Brunel et al. 2013).

1.5.4. Zinc Nanoparticles

Zn Nanoparticles were proved to be important antifungal agents which have showed deformation of fungal cell wall, and death of fungal hyphae through hydroxyl and superoxide radicals (Prasun patra and Goswami. 2012).Prominent inhibition of pathogenic fungi *Botrytis cinerea*, *Penicillium expansum* and was evident with ZnO NPs of 70 nm size. The ZnO Nanoparticles are also involved in restriction of the conidial development, conidiophores and leading to restriction of fungal hyphae (He et al. 2011).

1.5.5.Nano composites

Composite films have shown better inhibitory action on several fungal species wherein the composite films of Pullulan and Silver Nanoparticles showed strong inhibitory action on the

sporulation of *Aspergillus niger* (Pinto et al. 2013). Almost, 100% growth inhibition was observed in the case of *Pythium ultimum,Colletotrichum gloeosporioides, Magnaporthe grisea* with the application of Nanocomposites. The Nano sized silica –silver composite showed improved inhibition of various plant diseases (Park et al. 2006). It is interesting to observe that at 10 ppm concentration *Rhizoctonia solani* was inhibited whereas *Bacillus subtilis, Rhizobium tropici, Pseudomonas syringae, Azotobacter chrococuum,* and *Xanthomonas compestris pv.vesicatoria* lethality was observed at at100 ppm concentration.

1.5.6. Chitosan Nanoparticles

Chitosan is the most abundant naturally occurring polysaccharide next to cellulose. It is made of randomly distributed β –(1-4) – linked D – glucosamine and N – acetyl –D – glucosamine. Chemically it is called as poly (1-4) – 2- amino -2 deoxy –D – glucan. It's a polycationic, polyaminosaccharide with many significant biological and chemical properties. It is biodegradable, biocompatible, bioactive, polycationic hydrogel, and contains reactive groups like OH and NH_2. So it is widely used in medicine, pharmacy and biotechnology. Chitosan has the capacity to increase membrane permeability *in vitro* (Aspden et al. 1997: Dumitriu and Chornet 1998) and in vivo (Takeuchi et al. 1996). It also possesses mucoadhesive permeability increasing property. Chitosan has the ability of insulin absorption across human intestine epithelial cells (Caco-2) without any injury (Artursson et al. 1994, Schipper et al.1996, 1997, 1999). In pharmaceutics it in used to prepare films, beads, intragastric floating tablets, microspheres and Nanoparticles (Berthold et al.1996; Felt et al.1998 , Calvo et al.1997, Illum 2001). Chitosan is also applied as a hemostatic agent in vascular surgery, tissue culture and tissue regeneration (Kolhe & Kannan 2003: Li et al. 2006)

Chitosan scaffolds utilized in tissue engineering (Madihally & Matthew 1999). The desirable biological properties of chitosan enabling it to use in biomedical and drug delivery applications, chitosan Nanoparticles showed high cytotoxic activity towards tumour cells but no adverse effects on normal human liver cells (L-02) (Qi et al. 2005). High sorption capacity and antibacterial activity also showed by chitosan Nanoparticles (Qi et al. 2004). The polycationic nature of chitosan showed higher affinity with negatively charged biological membranes and site specific targeting *in vivo* (Qi et al. 2004). Particle size of the Nanopaticles of the chitosan Nanoparticles also increases their antitumour efficacy when applied as intravenous injection (Qi et al. 2005). *In vivo* efficacy also greatly increased due to the small size of the Nanoparticles (Qi & Xu. 2006).

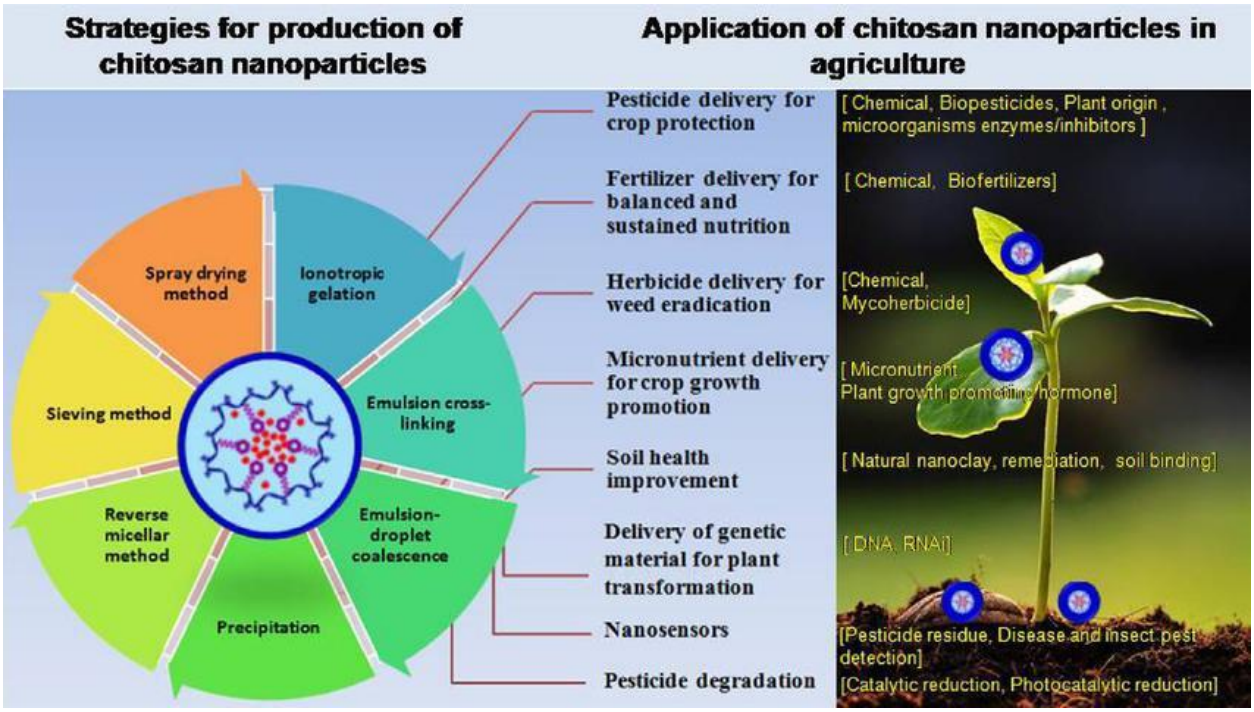

Fig 1.2: Applications of chitosan nanoparticles in agriculture

Due to its to its hydrophilic properties of proteins and peptides, chitosan is an effective drug carrier of hydrophilic components with excellent biodegradable biocompatible properties (Agnihotri et al. 2004). Inspite of its characteristic features chitosan is not completely soluble in water but soluble in dilute acidic solution. The rigid crystalline structure of the chitosan and the deacetylation which decreases its application to bioactive agents such as gene, peptide and drug carriers. Water soluble chitosan is easily soluble in neutral aqueous solution. The amino groups which are positively charged interacts with the negatively charged phospholipid components of plasma membrane and disrupts it, causes the leakage of cellular contents which ultimately leads to the death of the cell (Garcia-Rincon et al. 2010). Chitosan stops the growth of fungi on binding to trace elements by making nutrients unavailable for its development (Roller and Covill 1999). Chitosan also enter through penetration of the fungal cell wall and interacts with its DNA and affect the production of important enzymes (Sudarshan et al.1992: Kong et al. 2010).

1.5.6.1. Harpin – Elicitor protein involved in PCD of Plants

Harpin, the *hrp*-encoded elicitor of the hypersensitive response, was first isolated from *E. amylovora* ($harpin_{Ea}$;) (Wei et al.1992) and later from *P. syringae* pv. *syringae* ($harpin_{Pss}$;). (He et al.1993) The amino acid sequences of the two proteins are not similar, but they still have structural features in common. They are glycine-rich without any cysteine residues ; lack N-terminal signal sequences; hydrophilic ; and are heat-stable. Secretion of harpinPss has been shown to be dependent on the *hrp* encoded secretion system (He et al.1993). Since then, several harpins were isolated from *Pseudomonas, Xanthomonas, Ralstonia, Pantoea, Xyllella* etc. Harpins are effector proteins secreted by TTSS (Type 3 secretion system) of bacterial pathogen. Although harpins were originally defined as elicitors of HR, some other biological activity e.g induction of disease resistance has been reported (Jain et al. 2008). Harpins are known to possess multifunctional properties viz., enhanced growth and photosynthetic performance in plants, resistance against broad range of pathogens like viruses, bacteria, fungi and repelling insects. Because of these properties harpin was commercialized under trade name “Messenger”.

Beside the important biological activities harpins also attract considerable interest due to their potential application as pesticides. Since harpins do not directly interact with the disease causing organism, pathogens are not expected to develop resistance to harpins. As harpins are biodegradable and have no adverse effects on human health, use of harpins can substantially reduce use of more toxic chemical pesticides. The correlation of structure with activity in harpins may lead to development of improved engineered pesticides.

1.5.7. General Classification of Nanoparticles:

Based on the source of constitutents in the preparation of Nanoparticles, these are broadly categorized into eight types. They are Quantum dots, Nanocrystalline silicon, Photonic crystal, Liposomal, Gliadin, Polymeric, Solid Lipid Quantum, Metal Nanoparticles.

1.6. Synthesis of Nanoparticles

The Nanoparticles in general are prepared from variety of the natural/artificial materials i.e.,DNA, RNA, Proteins, Carbohydrates and Synthetic Polymers. The very commonly used methods for polymer based Nanoparticles include i) Polymerization of monomers ii) Dispersion of preformed polymers; and iii) Ionic gelation. Among these methods, Dispersion of performed polymers is used for synthesis of biodegradable Nanoparticles and Polymerization of monomers is utilized when the material is to be loaded is dissolved in the mixture and the Nanoparticles are prepared. The most routinely used method for synthesizing Nanoparticles with biodegradable compounds is ionic gelation method which is also referred to as coacervation method.

1.7. CHARACTERIZATION OF NANOPARTICLES

Characterization of Nanoparticles is crucial step as it confirms the morphological features of newly synthesized Nanoparticles. Further, it allows to know more about the controlled release of Nanoparticles and the methods employed for characterization of Nanoparticles include, Scanning Electron Microscopy (SEM), Transmission Electron Microscopy (TEM), Atomic Force Microscopy (AFM), X-ray Diffraction (XRD), Dynamic Light Scattering (DLS), Attenuated Total Reflectance Infra Red Spectroscopy (ATRIR), Fourier transform Raman Spectrometery (FTRS), Ultraviolet-Visible Spectroscopy (UV-Vis), Nuclear Magnetic Resonance (NMR),

Dynamic Light Scattering (DLS), N_2-Sorpometery, GC-Mass Spectrometery, Rheometric Analysis and Electron paramagnetic resonance spectrometery (ESR).

- **Transmission Electron Microscopy: TEM** allows the user to identify the 3-dimensional phase arrangement, crystal pattern and size distribution of the Nanoparticles/materials.

- **Scanning Electron Microscopy:** SEM allows identifying the external surface morphology and size distribution of the synthesized Nanoparticles.

- **Atomic Force Microscopy: AFM** visualizes the surface morphology of Nanoparticles in 2D and 3D as well as in obtaining average grain size.

- **X-ray Diffractometry :** The phase arrangement in the newly synthesized Nanoparticles or Nanomaterials is determined by XRD approach.

- **UV-visible spectrophotometry:** This method helps user to know more about the formation of Nanoparticles during the reaction and also facilitate the user in monitoring the reaction involved in Nanoparticles syn.

- **Attenuated Total Reflectance Infra Red Spectroscopy:** The ATR-IR reveals the functional groups in the novel Nanomaterials and allows the user to study the interaction of compounds that are present in the mixture of Nanoparticles formulation.

- **Fourier Transmission Raman spectrometry:** This procedure will allow the user to identify the nature of organic functionalities that are present around the Nanoparticles.

- **Zetasizer :** To detect the surface charge potential of the synzed Nanoparticles, zetasizer plays a crucial role in Nanoparticles characterization.

- **Nuclear Magnetic Resonance Spectrometry:** The NMR spectrum of Nanomaterials provide the data containing specific organic molecules that are interacting with Nanoparticles and also facilitate in identifying the complete reaction process used in the synthesis of Nanomaterials.

- **Dynamic Light Scattering machine and N_2-sorptometer:** These tools provide the details of size distribution and external surface of the Nanomaterials.

- **GC-Mass / EPR spectrometer:** For analyzing chemical components and magnetic properties of newly synthesized Nanoparticles.

- **Rheometric Analysis:** This method provides a complete information about Nanoparticles formation and assembly process.

With this background on utility of Nanoparticles, we have come up with the following objectives

Objectives:

- **Synthesis of harpin biofunctionalized nanoparticles and study of physicochemical**
- **To decipher the efficacy of harpin loaded chitosan nanoparticles and gold adsorbed Properties nanoparticles inducing Hypersensitive Response (HR).**

  -Biochemical and histochemical assays to confirm HR

  -Molecular assay confirming HR.
- **To study the localization of nanoparticles.**

Materials and Methods

2.1. Expression and purification of harpin$_{Pss}$

Harpin$_{Pss}$ was prepared as described earlier by (Sripriya et al. 2009**)**. The *hrp*Z gene (1020 bp) encoding full length harpin$_{Pss}$ was cloned under *Nde* I and *Xho* I sites of pET 28a vector (Novagen). *E. coli* BL 21 (DE3) cells transformed with pET28a-*hrp* Z were grown in LB broth containing Kanamycin (50 µg/mL) to OD 600~0.5 and induced with 1 mM IPTG. Following induction of three hours, all the cells were centrifuged and the pellet was collected washed and resuspended in 10mM sodium phosphate buffer (pH 7.5) and was soincated using Bandelin MS-72 Probe with a one minute pulse on thirty second pulse off for seven cycles. The sonicate was boiled for 10 min, then centrifuged at 18,000 *g* for 20 min to remove cell debris and the supernatant was loaded on to Ni-NTA column (Sigma Aldrich,USA). Protein was eluted with 200 mM imidazole in phosphate buffer, after washing the column with 20 mM imidazole in the same buffer and then dialyzed extensively against 10mM sodium phosphate buffer (pH 7.5). The dialyzed protein was concentrated using 10 kDa cut off membrane filter (Millipore,USA) followed by SDS-PAGE to check protein purity .the concentration of the was estimated according to (Bradford 1976).

2.2. Preparation of chitosan nanoparticles (CS-NPs)

Water soluble CS (Chitosan chlorhydrate (MW: < 200 kDa, DD 90%), a gift from Mahtani Chitosan (India), was dissolved in deionized water to prepare 1% (w/v) CS solution. To prepare the nanoparticles, 0.22% CS solution was flush mixed with 0.07% TPP (Loba Chemie Pvt. Limited, India) and the formation of chitosan-TPP NPs started spontaneously with the incorporation of TPP solution into CS solution under magnetic stirring at room temperature. Harpin$_{Pss}$-loaded CS-TPP NPs were obtained upon the

addition of a 0.07% TPP to 0.22% CS solution containing harpin (30 ng/mL) stirred at room temperature. During the incoroporation process, harpin molecules are entrapped/embedded in the chitosan-harpin nano-matrix, with some harpin molecules also adsorbing at the particle surface. The NPs were collected by centrifugation at 1,12,000 *g* on a 10 µL glycerol bed for 1 h and supernatants were discarded.

2.3. Synthesis and bioconjugation of gold nanoparticles (AuNPs)

Tetrachloroauric acid ($HAuCl_4$) (sigma-aldrich-USA) was reduced by citrate in the production of gold nanoparticles (AuNPs) 20 ml of 1.0 mM $HAuCl_4$ taken into a 50ml beaker and heated to its boiling point. trisodium citrate dihydrate (sigma-aldrich-USA) 2ml of 1% solution was mixed to the boiling solution. The citrate reduces the gold solution and a wine red colour was formed, which is the indication of formation of citrate surface coated gold nanoparticles (Frens 1973). The presence of citrate ions on the surface of gold nanoparticles limit particle growth and creates a stable colloidal dispersion. The solution was brought down to room temperature with a negative surface charge. Then 1ml of citrate capped (AuNPs) were conjugated with 70µg/ml of harpin under magnetic stirring. The same procedure was followed for bioconjugation of BSA. The positvely charged gold nanoparticles synthesized during the preparation of nanorods through seed mediated method. The solution was prepared by 0.2 M Cetyltrimethyl ammonium bromide of 5ml to 0.0005 M $HAuCl_4$ and Chilled 0.01 M of 0.6 ml was added to the solution (Tiwari et al. 2010). A brownish yellow solution observed stirred for few minutes and stored at room temperature. Colloidal stability of CTAB encapsulated AuNPs obtained by the addition of 0.1ml of 50ug/ml of harpin and BSA.

The resulted bioconjugated nanoparticles resulted with the positive interfacial surface charge.

2.3.1 Purification of AuNPs.

The citrate capped AuNPs and bioconjugated BSA and harpin was purified by the process of centrifugation at 10,000g for 20 min. The excess ions were removed by washing thrice by Millipore water. The same procedure followed for the CTAB encapsulated AuNPs and bioconjugated BSA, harpin. All the purified nanoparticles were stored at 4^0C in the dark.

2.4. Physicochemical characterization of harpin-loaded CS-NPs

2.4.1. Scanning Electron Microscopy (SEM)

The surface morphology and particle size of the sample is determined by SEM FEIXL 30 ESEM (Philips) operated at 20 KV. 0.5 mm x 0.5 mm clean square glass slide is cut and placed on the stub with carbon double sided sticky tapes. Place 2µl of the sample and spread all over the glass slide with the pipette manually and air dry the sample. Air dry specimen in dust free region at room temperature for one hour and covered with gold in sputter coater.

2.4.2. Trasmission electron microscopy (TEM)

Protein conjugated, unconjugated gold nanoparticles were synthesized for electron microscopy dimensions and air dried small aliquots of sample solution and placed on carbon coated carbon grids. The air dried grids were examined using Transmission electron microscopy (FEI TECNAI G^2 S-TWIN, 200kV, Netherlands). Electron diffraction patterns were stuidied from a particular area for conjugated and unconjugated protein nanoparticles.

2.4.3. Atomic Force Microscopy (AFM)

For measurement of particle size, of freshly prepared harpin-loaded CS-NPs,and chitosan nanoparticles. Atomic Force Microscopy was used. A 0.5 mm x 0.5 mm clean square glass slide is cut and 10µL sample was placed in a dust free region and evenly dispersed using a spin coater for one hour. The SPA- 400 was utilized to take images and recorded at different resolution. Size was analyzed.

2.4.4. UV-visible spectrophotometry

UV-visible absorption of the samples were recorded by means of 1 cm path length rectangular quartz cells through an absorption spectrophotometer (Shimadzu UV-vis 1800) and analyzed by uniprobe software.

2.4.5. EDAX- Spectroscopy

Energy dispersive x-ray spectroscopes uses the photon nature of light. A measurable x-ray voltage pulse can be made by a photon within the x-ray range. The output of an ultralow noise preamplifier connected to the low noise makes a statistical measure of the respective quantum energy. A multichannel analyzer counts a large number of such pulses which are digitally recorded and a complete image of the x-ray spectrum can be made simultaneously. To analyze the spectrum a semiconducted material is used to detect the x- rays with processing electronics. The gold solution was coated onto carbon film and examined using an EDAX- spectrometer (S-3400 N, Hitachi).

2.4.6. Silver staining

The gel was fixed with 50% methanol, 12% acetic acid and 0.05% HCHO. Incubated for 2 hours or overnight, washed with 35% ethanol 3 times each of 30 min. Then the gel was sensitized with 0.2%. N $a_2s_2o_3$ for 10 min and washed with double distilled water for

three times each of 5 min. Incubated for 20 min in $AgNO_3$ solution containing 0.2% $AgNO_3$ and 0.076% HCHO. After incubation, gel was washed with double distilled water twice (at least one minute for each wash). The gel was developed by placing in 6% NaoH and 0.05% HCHO. Then the gel was kept in stopping solution containing 50% methanol and 12% acetic acid until the bands were visualized.

2.4.7. Flocculation assay

The minimum amount of protein required to saturate the surface of nanoparticles was optimized by flocculation assay. Serial dilutions of protein solution were made and 0.1 ml of each dilution was added to 1 ml of colloidal gold solution. After 30 min 0.1 ml of 10 % NaCl solution was added and flocculation was induced. The amount of protein necessary to prevent the flocculation was determined by measuring the absorption at 520nm**.**

2.5. Evaluation of harpin encapsulation and *in vitro* release

Harpin-loaded CS-TPP NPs were separated from the aqueous protein suspension medium by ultracentrifugation at 1,12,000 *g* at 4^0C for 60 min. Supernatant from the centrifugation was carefully collected and protein content in the clear supernatant was measured by eosin-Y dye binding method, reading the absorbance at 536 nm (Waheed and Gupta., 1999). Samples were analyzed at each time interval in triplicates. The harpin loading capacity (LC) of the NPs and their association efficiency (AE) were calculated.

$$\% \ \mathbf{LC} = 100 \times (\text{total protein} - \text{free protein}) / \text{nanoparticle weight})$$

$$\% \ \mathbf{AE} = 100 \times (\text{total protein} - \text{free protein}) / \text{total protein})$$

For harpin release studies, the NPs in the form of sediment were transferred to a clean 5 mL eppendorf tube in 1 mL of phosphate buffer (pH 7.2) with horizontal shaking. The

sealed tube was placed in a 37^{o}C water bath. At diferent time points samples were centrifuged, the supernatant was taken and replenished by fresh buffer. Triplicate samples were analyzed. The amount of free- protein was measured in the clear supernatant by eosin-Y dye binding method taking the absorbance at 536 nm (Waheed and Gupta 1999).

2.6.Plant response studies

Nicotiana tabacum v xanthi was grown at 25^{0} C in environment-controlled green house. Forty day old tobacco seedlings were sprayed with 1 ml harpin-loaded CS-NPs, TPP (0.18 mg/ml), chitosan (2.2 mg/ml), harpin (11.11 ng/ml) and water on the third leaf of five different plants consisted of the five treatments in this study.

2.6.1.ROI production

Generation of reactive oxygen intermediates (ROI) was detected within 3h of spray treatment with harpin-loaded CS-NPs or controls. Into each leaf area previously sprayed with harpin, TPP, chitosan, CS-NPs ,100 µl of 0.4 mM DCFH-DA (Molecular probes) was injected as described by (Lu and Higgins 1998). 1 to 2 cm^{2} leaf tissues of these areas excised at 8 min after injection. The leaf tissues were observed using confocal microscope (Leica) with the excitation and emission wavelength of 488 nm and 525 nm respectively.

2.6.2. Determination of Programmed Cell Death (PCD)

Nuclear condensation was detected using 4,6- diamidino-2 phenyl-indole (DAPI) (Molecular probes), a membrane permeable dye that binds to DNA and stains condensed nuclei as bright spots, a feature observed in PCD. After 4 hours of treatment with harpin -loaded CS-NPs, TPP, chitosan, harpin 30 (ng/ml) and water, leaf slices were immersed in 1µM DAPI for 5 min in 0.5 M sucrose and examined under confocal microscope

(Leica) with the excitation and emission wavelength of 365 nm and 450 nm respectively (Govrin and Levine 2000).

2.6.3.Callose deposition assay

Leaf tissues of treated areas 1 to 2 cm^2 were excised and immersed in 5 ml of alcoholic lactophenol followed by boiling at 65^0 C for 15-30 min to clear the chlorophyll. The cleared leaves were washed in 50% ethanol then rinsed in water and stained for 30 min in 150mM K_2HPO_4 (pH 9.5) containing 0.01% aniline blue. Samples were placed in 50% glycerol and observed using confocal microscope (Leica) with the excitation and emission wavelength of 365 nm and 420 nm respectively (Adam and Somerville 1996).

2.7. Molecular Assay of HR induced by nanoparticles:

2.7.1. Isolation of RNA

Homogenization:1ml of Tri reagents (Qiagen) was added to 50-100mg of leaf tissue and homogenated, kept at room temperature for 5 min to permit the complete dissociation of Nucleoprotein complexes.

Phase separation: For every 1 ml of Tri-reagent 0.2ml of chloroform was added and vigorously shaken followed by stand alone at room temperature for 15 minutes. Centrifugation was done at 12,000g for 15 min at 4^0c.

RNA Precipitation: Transferred the aqueous phase to a fresh tube and stored the remaining interphase and organic phase at 4^0c. Added 0.5ml of isopropanol for 1ml of Tri reagent. Stored the samples at room temperature for 5-10 min. Centrifugation was done at 12,000g for 8 min at 4^0c. The pellet which was formed was stored.

RNA wash: The supernatant was removed. To this 1ml of 75% of 1 ml ethanol was added and 1ml of Tri reagent added and then centrifuged for 5 minutes at 7,500g at 4^0c. If pellet is floated and again it was sedimented at 12,000g.

RNA Solubilization: Air dried the pellet for 3 to 5 minutes and solubilised in RNase free water and incubated at 55-60^0c for 10-15 min. Purity of the dissolved pellet was measured by Thermoscientific Nanodrop (260/280).

2.7.2. RT-PCR Analysis

Plant gene expression was studied by reverse transcriptose PCR (RT-PCR). Amplification of a 18s rRNA served as an internal control. RNA was isolated (Invitrogen kit) from the treated third leaf of each plant from all the five different treatments as explained above. Reverse transcriptase was performed using oligo(dT) primers at 50^0C for 50 min and inactivated the reverse transcriptase at 85^0C for 5min. The first-strand c-DNA synthesized with 5µg of RNA which was treated with RNase-free DNAse. An equal volume of cDNA was amplified (30 cycles). The following gene specific primers (*PR1*; *PR2*; *PR3*; *Chia*-5; *hsr*; *hin*) were designed for RT-PCR amplification.

PR1: FP: 5'-GATGCCCATAACACAGCTCG-3'

RP: 5'TTTACAGATCCAGTTCTTCAGAGG-3'

PR2: FP: 5'-CTGCCCTTGTACTTGTTGGG-3'

RP: 5'-TCCAGGTTTCTTTGGAGTTCC-3'

PR3: FP:5'-GGTTCTATTGTAACGAGTGAC-3'

RP:5'-TTCTATGTAACGAAGCCTAGC-3'

Chia-5: FP: 5'-TCTCATGTTTCCTTCTCCGG-3',

RP: 5'-CAAAGTAACCTAGCAATCCTCTACC-3'

hsr: FP: 5'-TTACTAGACATCAGTTGGGAAG-3',

RP: 5'-TGTACTACACTGTCTACACGC-3'

hin: FP:5'-GAACGGAGCCTATTATGGCCCTTCC-3',

RP:5'-CATGTATATCAATGAACACTAAACGCCGG-3'

2.8. Rodamine isothiocyanate conjugatin of Harpin and BSA

For every 3µg of protein 1ng of RITC was added and dissolved in 20 µl of DMSO. The dissolved protein was dialized against milli-Q water for 2 hours (membrane with 10 kDa cut-off) to remove unconjugated protein. Milli-Q water was changed for 3 times with a 6h time interval. From the sample 1 µl was diluted to 10 ml and observed using spectifluorimeter (Shimadzu RF 5000). The conjugated protein after dialysis was used for conjugation of nanoparticles.

2.8.1. sectioning of the leaf sample for RITC studies

One to two square cm leaf tissues of treated leaf samples were sectioned using LEICA CM 1850 UV cryostat. Initially the leaf samples freezed in a freezing medium and embedded using modular tissue embedding system LEICA EG 1150 C. The sample was placed on the specimen disc and inserted the specimen disc in the specimen head. The samples were trimmed and then ultrathin sections of 4-5µ were cut with the help of cryostat and observed under LEICA Laser scanning confocal microscope TCS SP2 AOBS Germany at 540- 570nm.

2.9. Immunogold labelling of Harpin

The prepared gold nanoparticles were sprayed on the leaf and after 6 hours Leaf samples were fixed 0.25% glutaraldehyde and 3% paraformaldehyde at 4^0 C in 0.1 M phosphate

buffer (pH 7.2) for 2.5 hours followed by dehydration with ethanol series (graded) and embedded in London resin white acrylic resin . Leica Ultramicrotome was used to make thin sections (60-70 nm) and coated nickel grids were incubated for 30 min in PBS 5% (w/v) to block non specific binding. Incubated for 180 min with anti-harpin antibody raised in rabbit (diluted 1:250 with phosphate buffered saline (PBS) plus 5% (w/v) bovine serum albumin (BSA)) washed with PBS plus BSA 1% (w/v), the sections were incubated for 90 min with the secondary antibody (goat anti-rabbit IgG gold labelled (15 nm) diluted 1:50 with PBS plus 1% (w/v) BSA and 1% (w/v) Goat Serum). The sections were washed sequentially with PBS twice and 5 times using distilled water. Staining of ultrathin sections were carried out with uranyl acetate followed by lead citrate and observed in transmission electron microscope (TEM) (Prins et al. 2008).

Results

3.1. Expression and purification of harpin$_{Pss}$

The expression of Hrpz gene in *E.coli* BL 21 (rosettae) has yielded harpin protein encoding molecular weight of 34.7 kDa (Figure 3.1). The purified harpin protein was further used in preparation of nanoparticles (chitosan loaded and gold adsorbed) and also for histochemical studies.

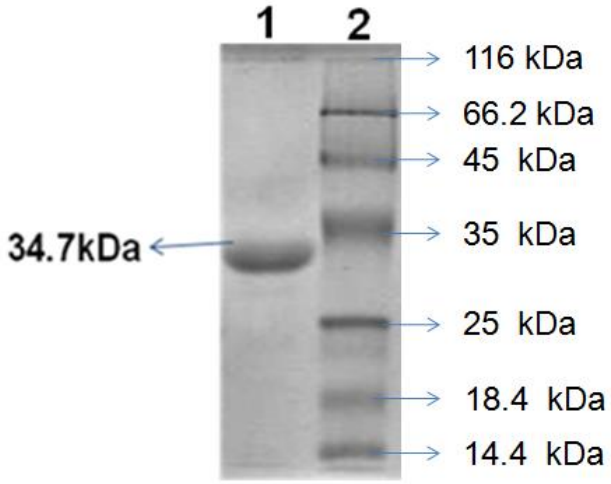

Figure 3.1: SDS – PAGE showing purified harpin$_{Pss}$ Harpin$_{Pss}$ expressed in *E. coli* BL 21 cells , purified on Ni- NTA column. The purified protein was applied onto the 12% SDS – PAGE to detect the molecular mass. Lane 1 indicates the purified protein and Lane 2 is protein molecular weight marker.

3.2. Preparation of chitosan nanoparticles (CS-NPs)

To entrap harpin in the CS matrix, variable volume of the TPP solution was incorporated into a fixed volume of the CS solution containing harpin under magnetic stirring. The harpin-loaded CS NPs formed immediately when polyanionic TPP was added CS-harpin solutions. Condensed and cross linking agent like TPP forms further hydrogen bonds with positively charged free amine groups on both harpin and CS molecules resulting in more packed in harpin-CS NPs.

The schematic representation of preparation of chitosan nanoparticles synthesis is depicted in the Figure 3.2:

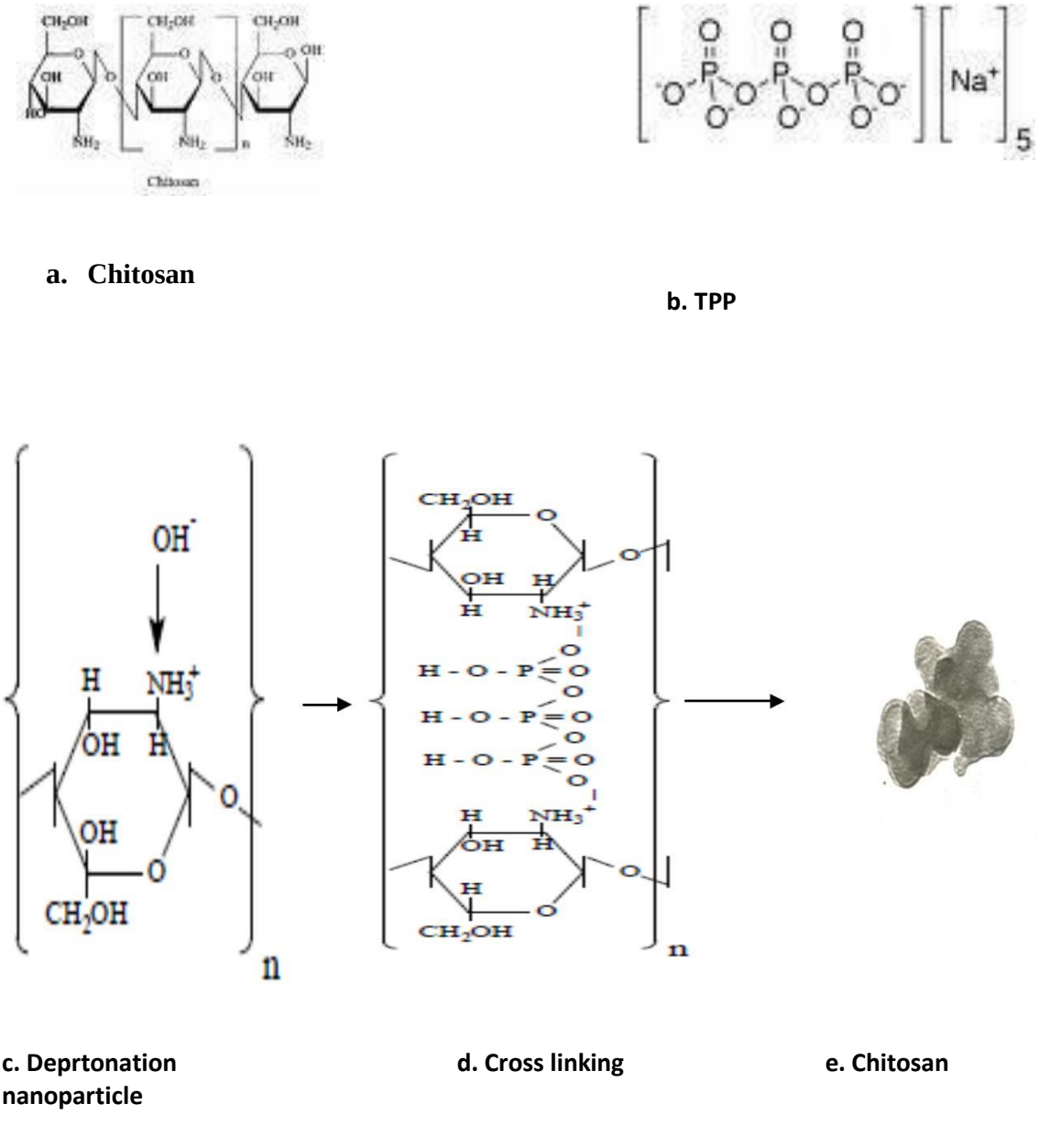

a. Chitosan

b. TPP

c. Deprtonation nanoparticle

d. Cross linking

e. Chitosan

Figure 3.2: Chemical structures of Chitosan (a), Sodium Tripolyphohsphate (b), interactions between Chitosan and TPP due to Deprotonation (c), Cross linking (d) leading to formation of chitosan nanoparticle (e).

3.3. Morphology and structure of chitosan nanoparticles and harpin loaded chitosan nanoparticles using SEM studies:

Scanning Electron Microscopy (SEM): The shape and surface of the NPs under the SEM indicated that the CS NPs and harpin-loaded CS-NPs were close to spherical, smooth and almost homogeneous (Figure 3.3).

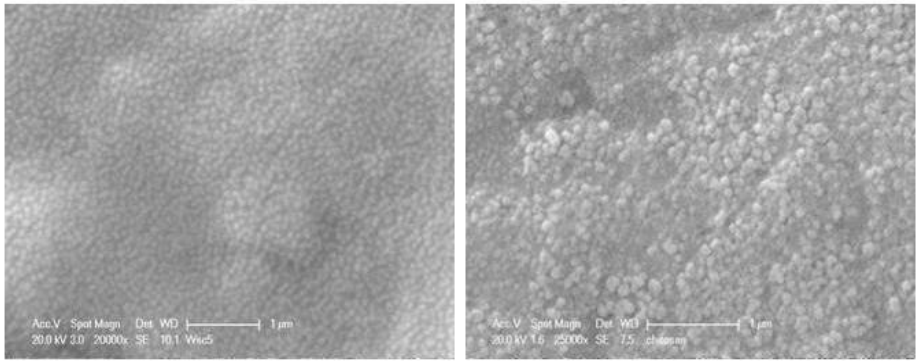

Figure 3.3. Scanning electron micrographs of harpin-loaded chitosan nanoparticles. Protein loaded chitosan nanoparticles (CS NPs) prepared at pH 5.2 with 30ng/ml of harpin by ionotropic gelation of chitosan with tripolyphosphate anions. Equal amounts of harpin and chitosan were pre-mixed before the addition of TPP. A) CS-NPs and B) harpin-loaded CS-NPs.

The Scanning Electron Microscopic studies clearly revealed the harpin loaded chitosan nanoparticles have showed increased size compared with the chitosan nanoparticles. The SEM images clearly reflect the aggregation of nanoparticles in both the chitosan nanoparticles and harpin laoded chitosan nanoparticles. The individual chitosan nanoparticle size was 228nm to 230nm whereas the harpin loaded chitosan nanoparticles was observed as 250nm. The increased size of harpin loaded chitosan nanoparticles might be due to the entrapment of harpin inside the chitosan matrix (Figure 3.3).

3.4. Synthesis and bioconjugation of gold nanoparticles (AuNPs)

The transmission electron micrographs of gold and conjugates were 13 nm in diameter and well dispersed in the solution. The panel A, B, and C indicates gold and citrate capped nanoparticles conjugated with harpin and BSA, whereas the Panel D, E, and F are gold- CTAB and harpin BSA conjugated nanoparticles. The citrate capped nanoparticles possess negative charge on their surface and CTAB capped gold nanoparticles possess a positive surface charge on the surface. The synthesized particles are uniform in diameter, spherical in shape and well dispersed (Figure 3.4). As the particles possess surface charges, they posses repulsive forces among them. Interestingly, all the various nanoparticles reported was found to be uniform that there was no observation of different shapes in all the TEM images.

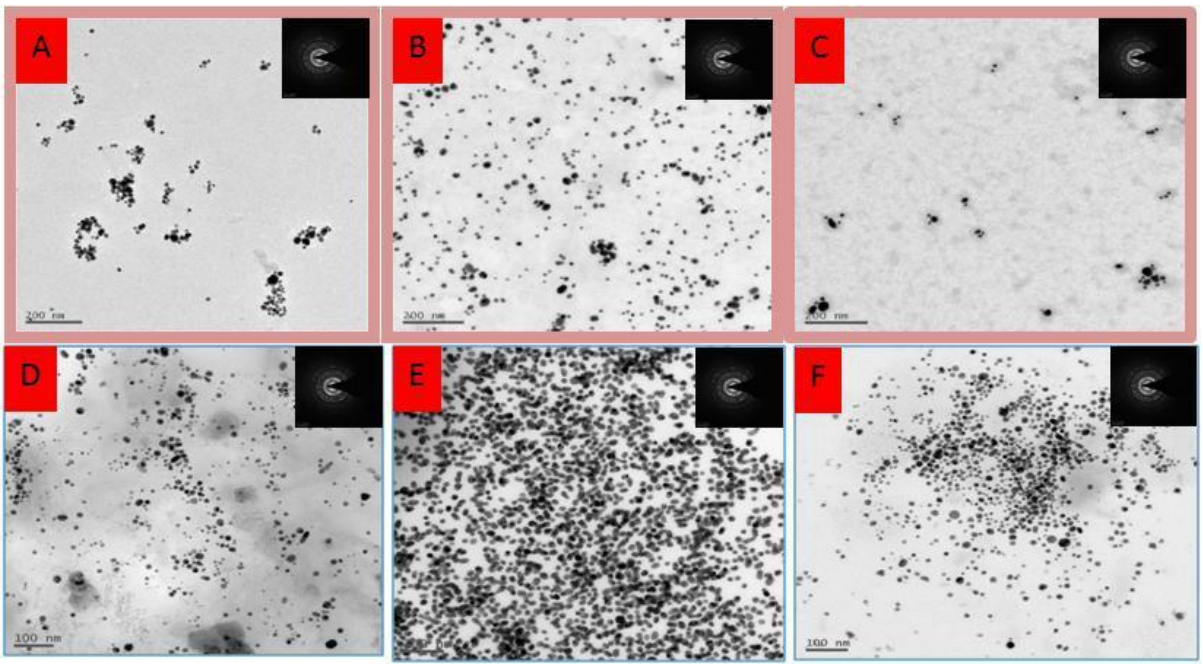

Figure 3.4: Transmission electron micrographs of gold nanoparticles a) Au-NPs; b) Au NP-BSA; c) Au NP- Harpin NPs; D) Au NPs-CTAB NPs; e) Au NP-CTAB-BSA NPs and f) Au-NP-CTAB-Harpin NPs

3.5.Atomic Force Microscopy (AFM)

The size analysis of the NPs, as analyzed by the atomic force microscope, revealed that the CS NPs have diameters of 228-288nm and the harpin-loaded CS NPs have 307-374 nm (Figure 3.5) indicating that there was increase in the size due to loading with harpin. The surface morphology of the NPs appeared to be smooth.

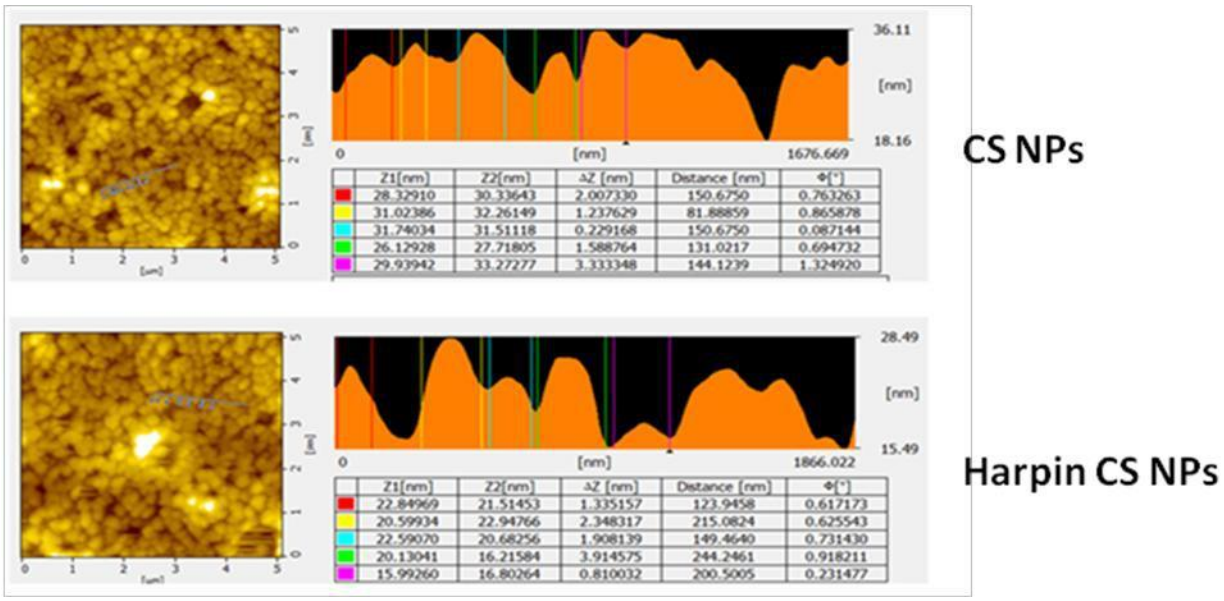

Figure 3.5: Surface display analysis of chitosan-nanoparticles (CSNPs) and harpin - loaded chitosan nanoparticles (Harpin CSNPs) The CSNPs/ Harpin CSNPs were dried on a glass slide in a dust free zone for 1 h and observed under atomic force microscope. The images were acquired at 5 x 5 µM resolution. Size of the nanoparticles was determined by taking the average of 5 particles.

3.6.UV-visible spectrophotometry

UV-Visible spectra of gold and conjugates: For each 1ml of gold solution100µl of 10 to 70µg/ml of protein solutions and 100µl of 10% NaCl was added and observed at 520 nm using UV visible spectrophotometer. 10 and 20µg/ml showed decreased absorbance and it is visible in the analysis compared with pure gold nanoparticles of absorbance at 520 nm which were correlated with the flocculation assay.

From 30µg to 70µg successively the absorbance got increased with the increased concentration of protein and a shift in the peak was observed from 520 nm to 523 nm in the case of 70 µg/ml of protein solution indicating that at this concentration the surface of gold nanoparticles were stabilized which already seen in the flocculation assay. Gold nanoparticles with 60 µg/ml of BSA also showed shift in the peak indicating that these

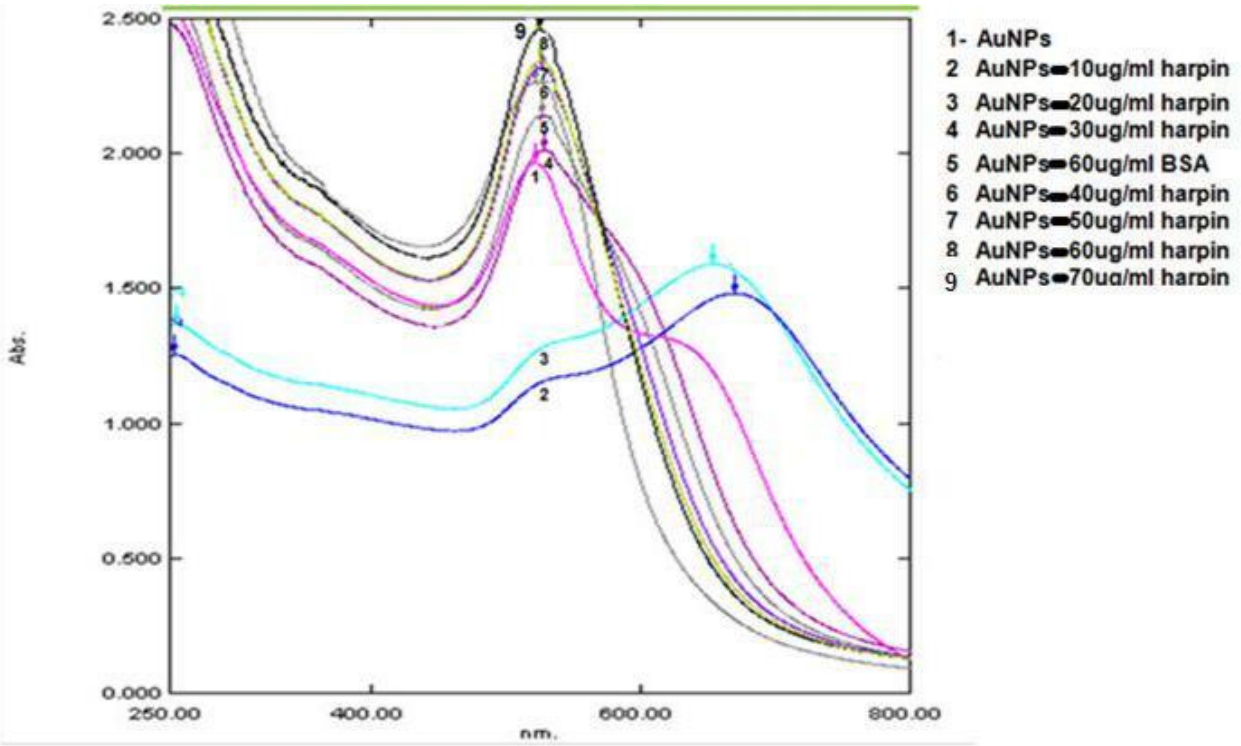

particles also surface stabilized with BSA.

Figure 3.6: UV- vis spectrum of AuNP's and AuNP's with concentrations of 10 to 70µg/ml.
The gradual shift in the peak of AuNP's with incresed concentrations from 10 to 70µg/ml observed indicating the conjugation of harpin protein with AuNP's. Increase in the absorbance was visualized with increasing concentrations of protein.

3.7. UV-Visible spectra of gold-CTAB and conjugates:

For each 1 ml of gold solution 100 ul of harpin protein having the concentrations 40 µg/ml, 50 µg/ml and BSA 40 µg/ml was mixed to this 100 ul of 10% NaCl was mixed and observed at 527 nm. A shift in the peak was observed in the case of harpin concentration of 50 µg/ml and BSA 40 µg/ml indicating that they are surface stabilized with these concentrations.

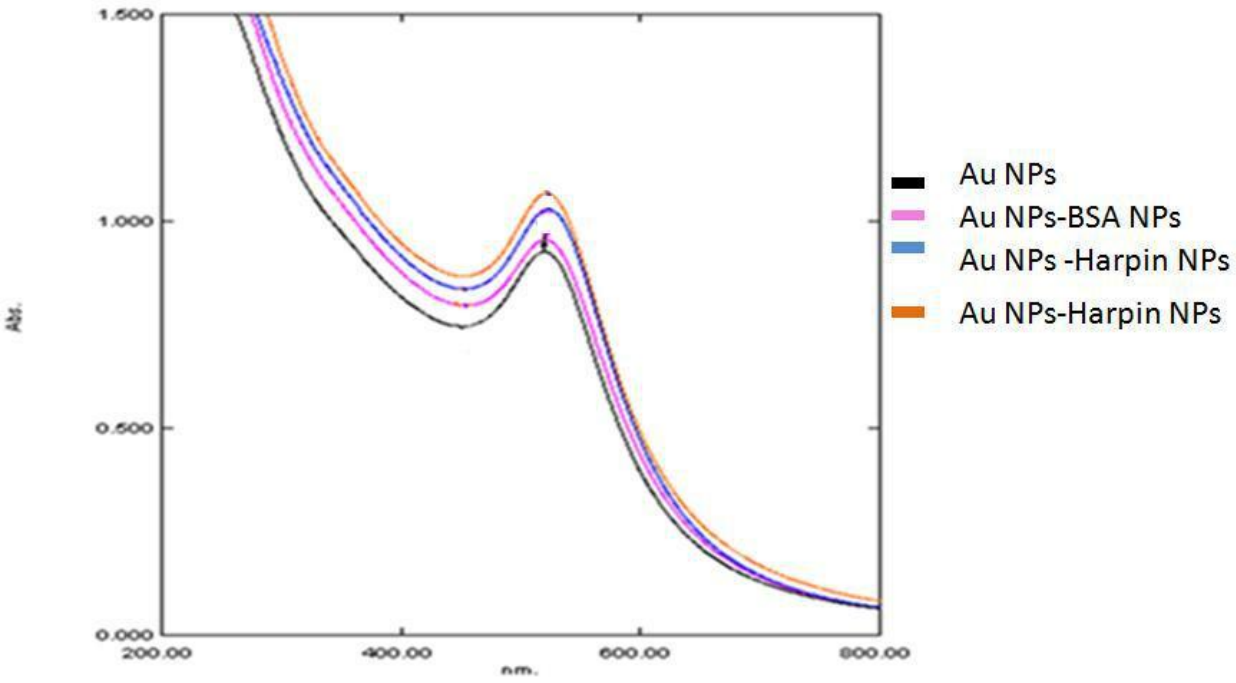

Figure 3.7: UV- vis spectrum of AuNP's and AuNP's with BSA (40µg/ml) and harpin of 40 and 50µg/ml.
The gradual shift in the peak of AuNP's with concentrations 40 and 50µg/ml observed indicating the conjugation of harpin protein with AuNP's. Increase in the absorbance was observed with increasing concentrations of protein.

3.8. Zeta Potential Studies for Size Determination

The Zeta potential of the gold nanoparticles prepared in the current study showed high zeta potential having greater stability and decrease in the potential indicates that protein is adsorbed on the particle surface. In the (Table 1.1) A,B,C, are citrate capped and negatively charged nanoparticles showing high zeta potential having greater stability and the increase in the potential indicates protein is adsorbed on the particle surface. In the (Table 1.1) 4, 5, 6 are Gold-CTAB-Nanoparticles showing positive zeta potentials and the decrease in the potential indicates protein adsorption on the nanoparticles surface. All nanoparticles are showing greater stability as their zeta potential was measured at 25^0C.

Zeta potential of Gold and Conjugates:

Sl.No	Nanoparticles	Zeta potential in mV
1	Gold nanoparticles	-31.4
2	Gold BSA-Nanoparticles	-17.3
3	Gold Harpin Nanoparticles	-24.1
4	Gold CTAB-Nanoparticles	37.3
5	Gold CTAB-BSA- Nanoparticles	34.4
6	Gold CTAB-Harpin-Nanoparticles	36.3

Table 1.1 Zeta potentials of Gold and their conjugates.

3.8 EDAX- Spectroscopy

3.8.1.The SEM and EDAX spectrum studies of gold nanoparticles

The prepared gold nanoparticles were examined using EDAX-spectroscopy which showed the presence of gold without any contaminants (Figure 3.8.1). The EDAX profile of gold and conjugates showed strong gold atom signals at 2.1, 9.4, 10, 11.3, 13.2 and weaker signals for carbon 0.1, oxygen 0.4 and sodium 1ke v.

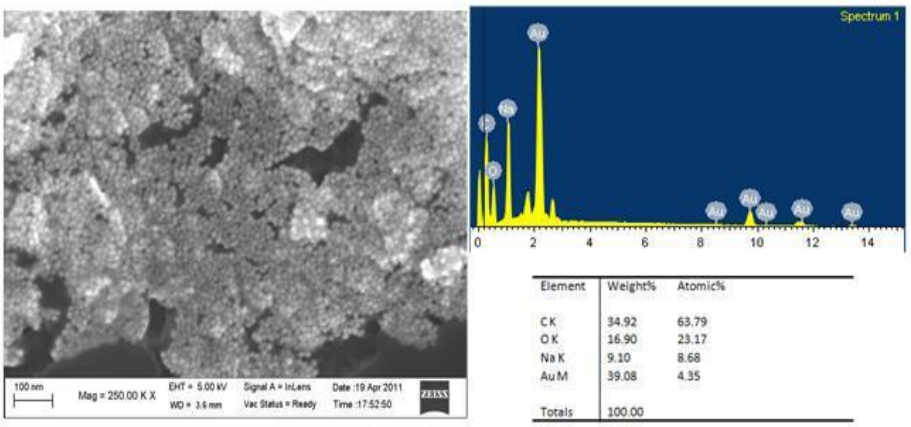

Figure 3.8.1: SEM and EDAX spectrum studies of gold nanoparticles

3.8.2. The results obtained from SEM and EDAX specturem of gold – BSA nanoparticles showed the presence of gold without any contaminants (Figure 3.8.2). The EDAX profile of gold and conjugates showed strong gold atom signals at 1.3, 2.1, 9.4 and feeble signals for carbon 0.1, oxygen 0.3 and sodium 1ke v.

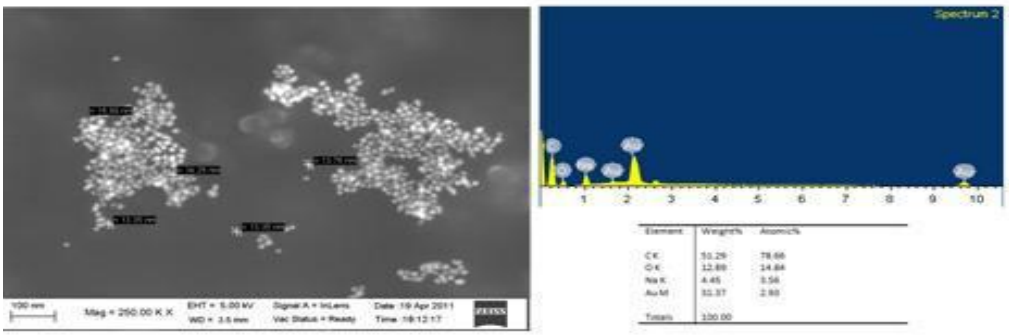

Figure 3.8.2: SEM and EDAX spectrum studies of gold- BSA nanoparticles

3.8.3.The SEM and EDAX spectrum studies of gold harpin nanoparticles

The prepared gold – Harpin nanoparticles were examined by using EDAX-spectroscopy which showed the presence of gold without any contaminants (Figure 3.8.3). The EDAX profile of gold and conjugates showed strong gold atom signals at 2.1, 9.4 and weaker signals for carbon 0.1, oxygen 0.3 and sodium 1ke v.

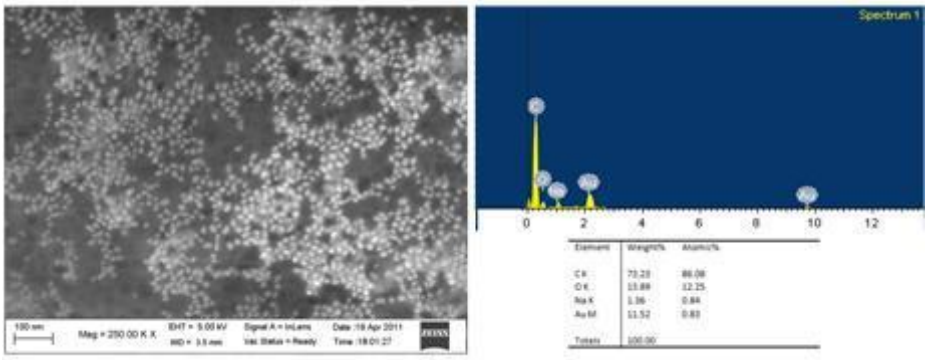

Figure 3.8.3: SEM and EDAX spectrum studies of gold harpin nanoparticles

3.8.4.The SEM and EDAX spectrum studies of gold CTAB nanoparticles

The prepared gold – CTAB nanoparticles were examined using EDAX-spectroscopy which showed the presence of gold without any contaminants (Figure 3.8.4). The EDAX profile of gold and conjugates showed strong gold atom signals at 1.3, 2.1, 8.3, 9.4, 10.1 and weaker signals for bromine 1.3, 0.1, oxygen 0.3 and sodium 1ke v.

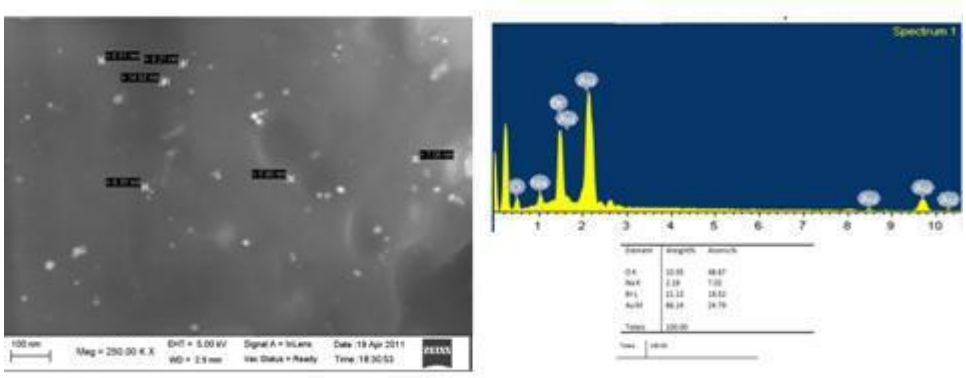

Figure 3.8.4: SEM and EDAX spectrum studies of gold CTAB nanoparticles

3.8.5. The SEM and EDAX spectrum studies of gold CTAB- BSA nanoparticles

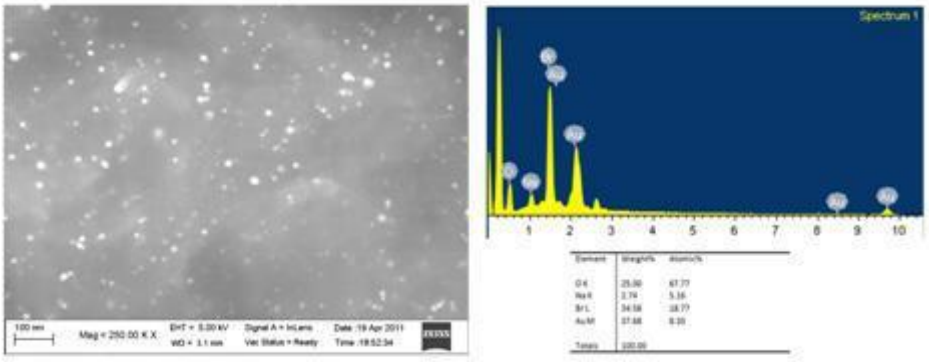

Figure 3.8.5: SEM and EDAX spectrum studies of gold CTAB- BSA nanoparticles

The synthesized gold-CTAB–BSA nanoparticles were examined using EDAX-spectroscopy which showed the presence of gold with no contaminants. The EDAX profile of gold and conjugates showed strong gold atom signals at around 1.3, 2.1, 8.3, 9.4 and weaker signals for bromine 1.3, oxygen 0.3 and sodium 1ke v.

3.8.6.The SEM and EDAX spectrum studies of gold CTAB- HARPIN nanoparticles

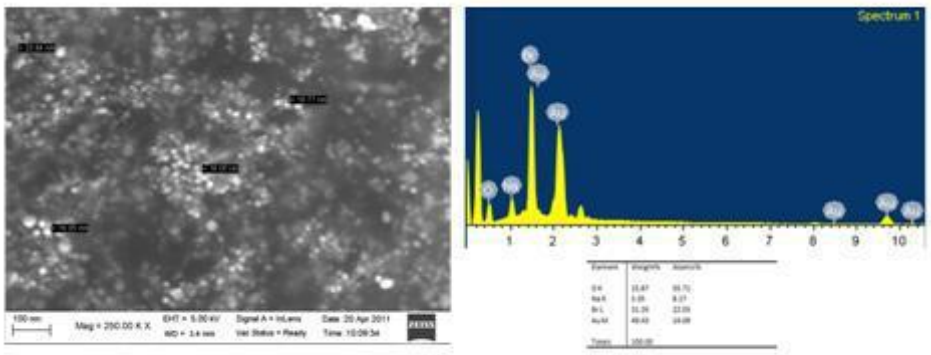

Figure 3.8.6: SEM and EDAX spectrum studies of gold CTAB- HARPIN nanoparticles

The synthesized gold-CTAB-Harpin nanoparticles were examined using EDAX-spectroscopy which showed the presence of gold with no contaminants. The EDAX

profile of gold and conjugates showed strong gold atom signals at around 1.3, 2.1, 8.3, 9.4, 10.1 and weaker signals for bromine 1.3, oxygen 0.3 and sodium 1ke v.

3.9. Silver staining

The protein adsorbed nanoparticles were heated at 100^0C for 10 minutes. 20ml of each sample was added onto 12% SDS – PAGE and electrophoresis was done. As the sample was heated the adsorbed protein was released from the nanoparticle and visualized as bands. Lane 2 is purified harpin of 34.7 kDa, the lane 5 and lane 8 conjugated with harpin protein released and appears as bands. Lane 3 is pure BSA ,lane 6 and lane 9 appears at the same level indicating that proteins are adsorbed on the nanoparticles surface.

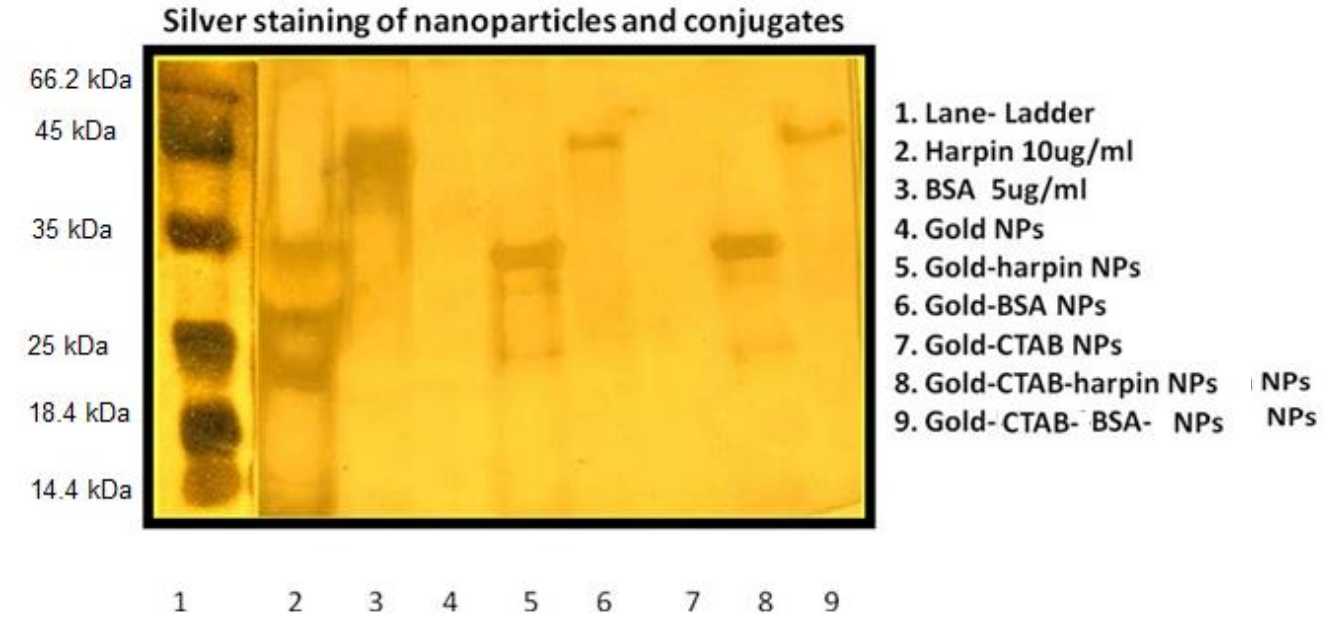

Figure 3.9: Silver staining of gold and its conjugates.

The gel was fixed with 50% methanol and 5% acetic acid , washed in 50% methanol for 10 minutes and washed in water for 10 minutes .The gel was sensitized with sodium thiosulphate and submerged with silver nitrate, formalin solution. The gel was developed

with sodium carbonate and formalin solution. 5% acetic acid was used as stopping solution. The gel was washed with water and preserved in glycerol.

3.10. Flocculation assay: In the flocculation assay for every 1ml of gold solution is added with different concentrations of proteins ranging from 10-70 ug/ml of 100 ul was added. To this solution 100 ul of 10% NaCl was added. Flocculation was observed in the 10 and 20 ug/ml of solutions the colour change was observed as a result of flocculation. The colour was blue as the solution obsorbs light at longer wave lengths. From there onwards the colour was slowly turned to deep wine red colour and in the 70 ug/ml of protein added sample showed a deep wine red colour indicating surface stabilized nanoparticles in the solution. The strong electrolyte which was added screens repulsive forces between the negatively charged citrate capped gold nanoparticles results in agglomerization of nanoparticles.

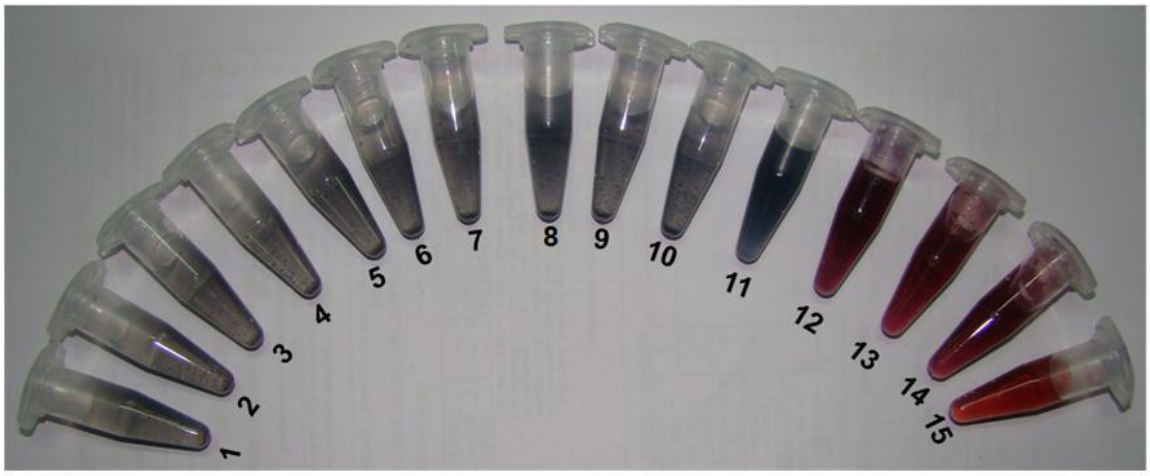

1,2,3,4,5,6,7,8,9,10,20,50,60,70,ug/ml and control

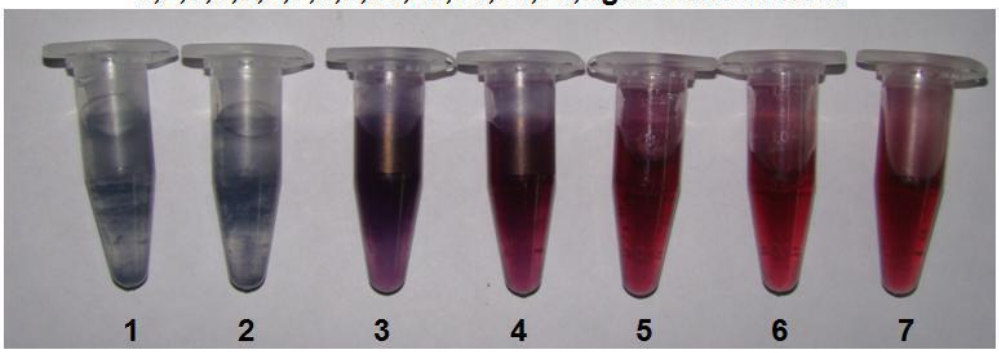

10,20,30,40,50,60,70ug/ml

Fig.3.10 Colorimetric detection of stable gold nanoparticles.To each 1 ml of harpin concentrations ranging from 1,2,3,4,5,6,7,8,9,10,20,50,60,70 µg/ml , 100 µl of NaCl was added and colour change was observed. Blue colour appeared starting from 1 to 60 µg/ml. Change of colour from blue to wine red was observed in the 70 µg/ml concentration indicating the formation of stable nanoparticles without any aggregation. Appearance of blue colour was an indication of aggregation of nanoparticles.

3.11. Evaluation of harpin encapsulation and *in vitro* release

The association efficiency of harpin with the CS NPs was 24%, while the loading capacity was 2.8% since we have used a very low concentration of harpin. The releasing kinetics revealed the slow release of harpin from the CS-NPs. Harpin release kinetics showed at around 33% of the entrapped harpin was released into the phosphate buffer in the first 30 min and reached to 57% in 60 min and further release was not observed even

after 24 h (Figure 3.11). These results indicate that the harpin was associated with the CS-NPs inside the core.

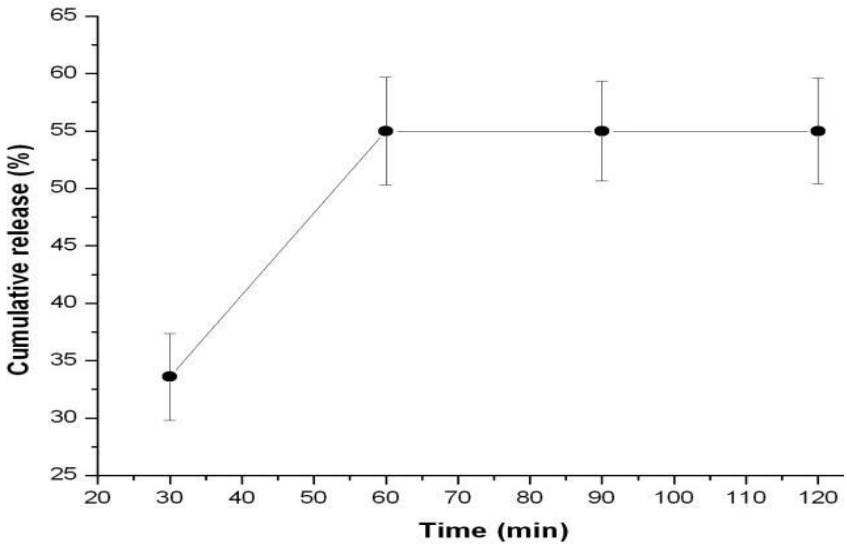

Figure 3.11. Release profiles of harpin loaded chitosan nanoparticles.

Nanoparticles were pelletized on the glycerol bed. Releasing kinetics of associated harpin from the CS-NPs was assessed after every 30 min at 37^0C in phosphate buffer at pH 7.2 (mean ± SD, n=3). The amount of protein release at specific time points was assayed and cumulative release % was calculated with respect to the initial loading capacity of the CS-NPs.

3.12.Plant response studies

3.12.1.Production of ROI in treated plants

One of the characteristic features of HR is production of reactive oxygen intermediates (ROI) and oxidative burst like O_2^-, H_2O_2 and HO which are toxic to producing cell and invading pathogens. ROI is involved in the generation of systemic acquired resistance, activation of defense related genes and cell death by oxidative damage. To assess the

intensity of oxidative burst, a fluorescent probe DCFH-DA was injected into each leaf area previously sprayed with harpin-CS-NPs and respective controls. The production of fluorescent compounds was detectable in the leaves treated with harpin-loaded CS-NPs, TPP, chitosan, harpin and water within 3 h (Figure 3.12). However, the intensity of fluorescence was much higher in the harpin-loaded NPs-treated leaves than in the TPP, chitosan, harpin and water-treated leaves. The results indicate a rapid and intense accumulation of ROI in harpin-loaded CS- NPs sprayed leaves resulting in an oxidative burst and consequential cell death.

3.12.2.Detection of nuclear condensation by DAPI

To examine whether ROI accumulating cells exhibited signs of PCD, we have observed a closely associated feature like nuclear condensation using DNA binding dye 4',6 – diamidino – 2 phenyl – indole (DAPI). Condensed DNA, apparent as bright DAPI stained spots, was distinctly visible in the leaves after 4 h of treatment with harpin-loaded CS-NPs compared to the TPP, chitosan, harpin and water sprayed leaves (Figure 3.12). These results indicate a strong and rapid induction of HR (a form of PCD) when harpin was sprayed on tobacco plants as harpin-loaded CS-NPs than pure solution.

3.12.3.Deposition of callose in treated plants

Callose is β, 1-3 glucan a polysaccharide regarded as a mechanical barrier which restricts the growth of pathogen by strengthening the host cell wall . Tobacco leaves treated with harpin-loaded CS-NP's treated region of the leaf sample showed many callose brilliant light blue dots under confocal microscope and scanty dots in the leaves treated with chitosan and harpin, indicating that harpin-loaded nanoparticles were working well in the plant system in mounting HR

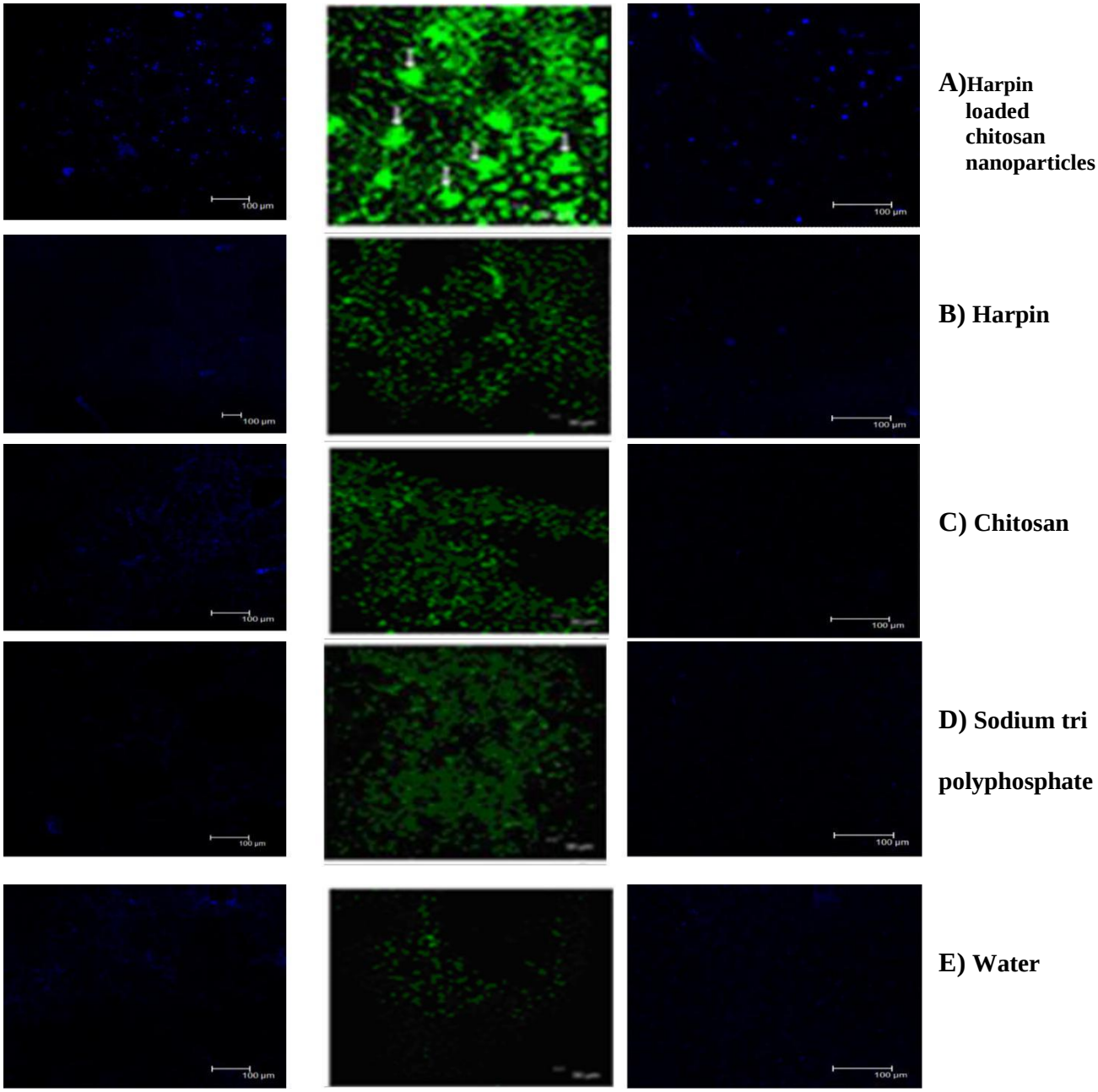

Figure 3.12. Induction of ROI, nuclear condensation and callose deposition in tobacco leaves sprayed with harpin-loaded chitosan nanoparticles. Confocal images of tobacco leaves sprayed with A) harpin-loaded chitosan nanoparticles, B), harpin, C), Chitosan, D) Trisodium polyphosphate and E) Water after 3 or 4 h of treatment.Samples were treated with aniline blue to detect callose depositon ,2,4,dichlorofluorescein diacetate to detect ROI and 4'-6- diamidino-2-phenyl indole to detect nuclear condensation respectively. Callose deposition (left panel) was recorded at an excitation wavelength 365nm and the emission wavelength 420nm, ROI formation (middle panel) at an excitation wavelength 488nm and the emission wavelength 525nm and nuclear condensation (right panel) visualized at an excitation wavelength 365nm and the emission wavelength 450nm.

3.13.Molecular Assay

3.13.1. RT-PCR analysis to determine HR due to foliar spray of CS-NPs

To examine whether the rapid generation of ROI and nuclear changes typical to a HR in harpin- CS-NPs sprayed plants coincided with the expression of HR-specific markers, wehave examined the expression of *hsr, hin* and *chia-5* genes. RT-PCR results showed a strong amplification of all the three genes with the expected products size of 618bp (*hsr*), 867bp (*hin*), and 1,015bp (*chia-5*) indicating the occurrence of HR at the molecular level (Figure 3.13.1) in the leaves sprayed with harpin-loaded CS-NPs. The plants treated with harpin also showed amplification of *hsr* and *chia-5* genes but, with much less intensity. The components used in nanoparticle preparation like TPP , chitosan when sprayed on tobacco plants, resulted in without expression any genes.

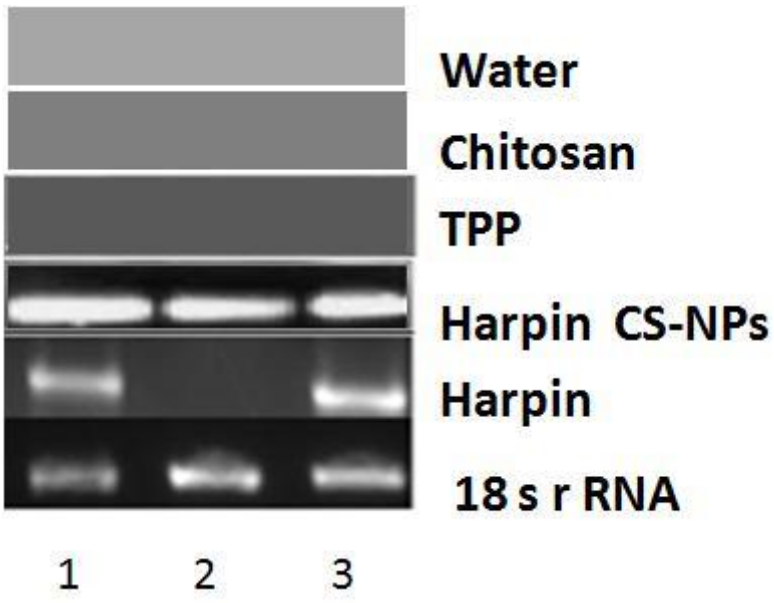

Figure 3.13.1. Expression of defense related genes in tobacco leaves sprayed with harpin-loaded chitosan nanoparticles. Each 1 mL of harpin, TPP, Chitosan, Harpin laoded chitosan nanoparticles sprayed on the tobacco plant. RNA was isolated from treated leaves after 6 hours of post treatment using TRIZOL reagent and c-DNA synthesized. Amplification of 18s rRNA was used as loading control. Lane 1 to 3 corresponds to *hsr, hin* and *chia-5* respectively

3.13.2. RT-PCR analysis to determine HR due to foliar spray of gold nanoparticles:

Each 1 ml of harpin, gold BSA nanoparticles, gold NPs, water, and harpin adsorbed gold NPs were sprayed on the well expanded tobacco leaf. After 6 hrs of post treatment RNA was isolated and c DNA was synthesized. A strong amplification of pathogen related genes were observed in the case of harpin adsorbed gold nanoparticles. Scanty expression of *PR-1,PR-2,* was exhibited in harpin treated sample. No other treatments showed expression of defense realted genes. This clearly indicates that harpin adsorbed nanoparticles worked well in the tobacco and upregulated pathogen related gene expression. PR-1 a marker gene for SAR and PR-2 belongs to a family of β 1-3 endoglucanases, *chia-5* acts against nematodes and herbivorous insects and hin a marker gene for SAR.

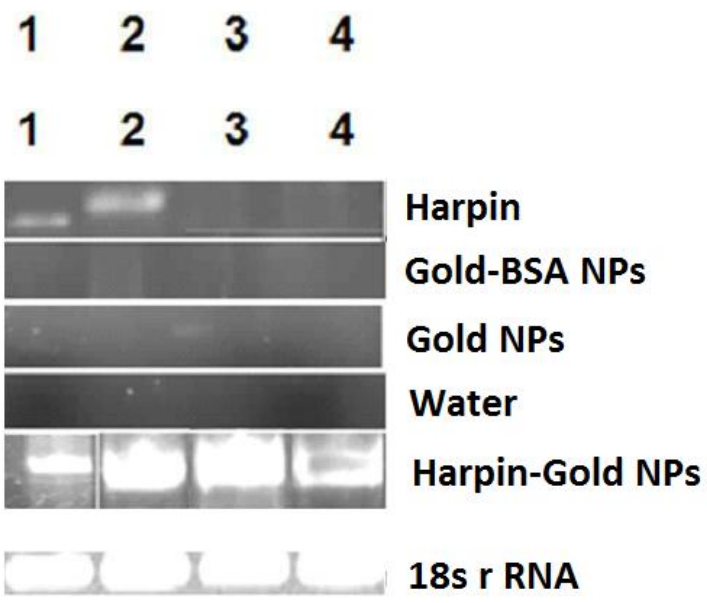

Figure 3.13.2. Expression of defense genes upon treatement with GOLD nanoparticles. Each 1 ml of harpin, gold-BSA NPs, gold NPs, water, harpin conjugated gold nanoparticles sprayed on the tobacco plant. RNA was isolated from treated leaves after 6 hours of post treatment using TRIZOL reagent and c-DNA synthesized. Amplification of 18S rRNA was used as loading control. Lane 1 to 4 corresponds to *PR-1,PR-2, Chia-5, hin* respectively.

3.13.3. RT-PCR analysis to determine HR due to foliar CTAB gold nanoparticles:

Each 1 ml of Gold-CTAB-BSA nanoparticles, gold CTAB NPs, water, and harpin adsorbed gold NPs and harpin were sprayed on the well expanded tobacco leaf. After 6 hrs of post treatment RNA was isolated and c DNA was synthesized. A strong amplification of pathogen related genes were observed in the case of harpin adsorbed gold nanoparticles. Scanty expression of *PR-1, PR-3, chia-5, hsr* was exhibited in harpin treated sample. No other treatments showed expression of defense realted genes. This clearly indicates that harpin adsorbed nanoparticles worked well in the tobacco and upregulated pathogen related gene expression. *PR-1* a marker gene for SAR and *PR-2* belongs to a family of β 1-3 endoglucanases, *chia-5* acts against nematodes and herbivorous insects and hin, hsr a marker gene for SAR, *PR-3* belongs to a family of endochitinases which acts against fungal members.

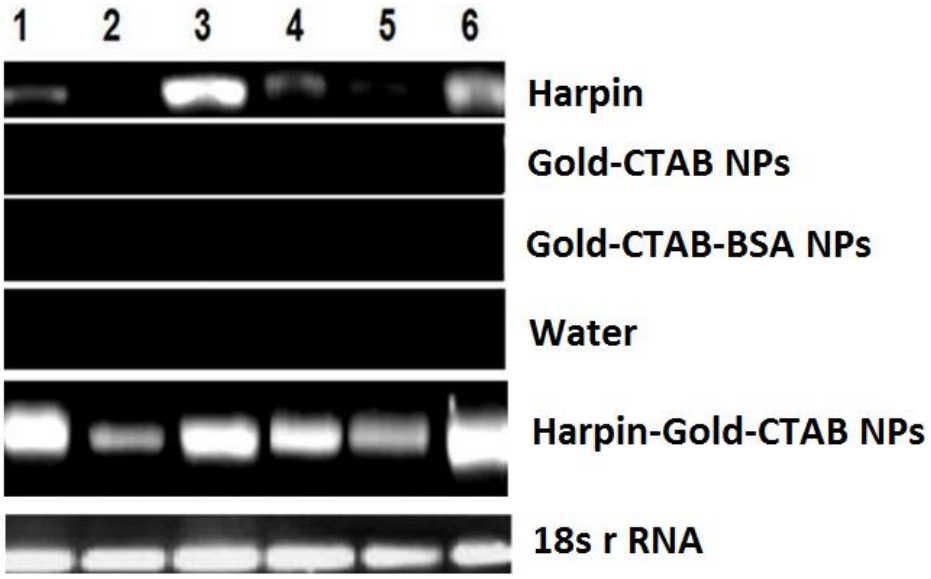

Figure 3.13.3: **Expression of defense genes upon treatement with GOLD/CTAB nanoparticles.** Each 1 mL of harpin, CTAB- BSA NPs, CTAB NPs water, harpin conjugated CTAB- gold nanoparticles sprayed on the tobacco plant. RNA was isolated from treated leaves after 3 hours of post treatment using TRIZOL reagent and c-DNA synthesized. Amplification of 18S rRNA was used as loading control. Lane 1 to 6 corresponds to *PR-1,PR-2, PR-3 , Chia-5, hin,* hsr respectively.

3.14. Nanoparticle Localization studies with RITC

The gold nanoparticles which were prepared were sprayed on the tobacco plant and after 6 hrs of time interval ultra thin sections were made with cryostat and observed under confocal microscope. The confocal imaging of control gold- CTAB NPs, gold NPs doesn't show any flourescence as the particles are not conjugated with RITC. Here no protein was used in the preparation of nanoparticles as a result fluorescence doesnt't occurred in the above said treatments.

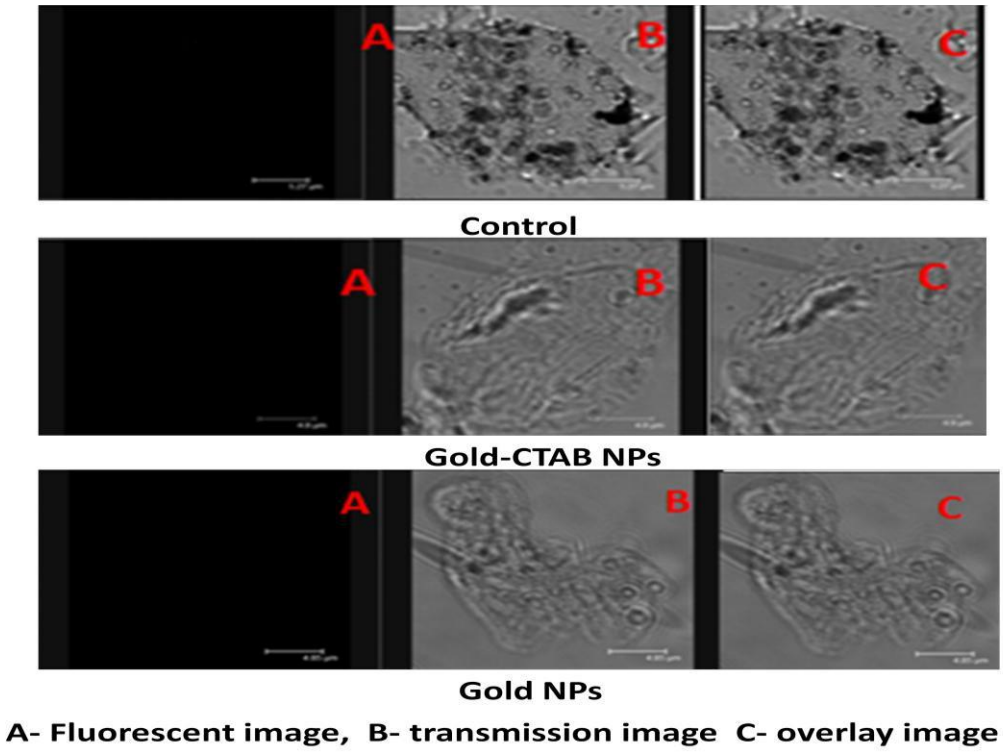

Figure 3.14: Confocal imaging of nanoparticles: Confocal images of control ,gold-CTAB NPs and gold NPs. The nanoparticle solution and water sprayed on the leaf of tobacco plant. A is the fluorescent image, B is the transmission image, C is the superimposed images. Fluorescence was not observed in the images A&C indicating that nanoparticles were not bioconjugated with proteins.

The proteins BSA and harpin were conjugated with RITC and these proteins were utilized for the preparation of nanoparticles. The pictures of BSA harpin and gold-CTAB-BSA nanoparticles showed fluorescence in the fluorescent image. The overlay image also shows red coloured fluorescence indicating that the BSA and harpin are conjugated with RITC.

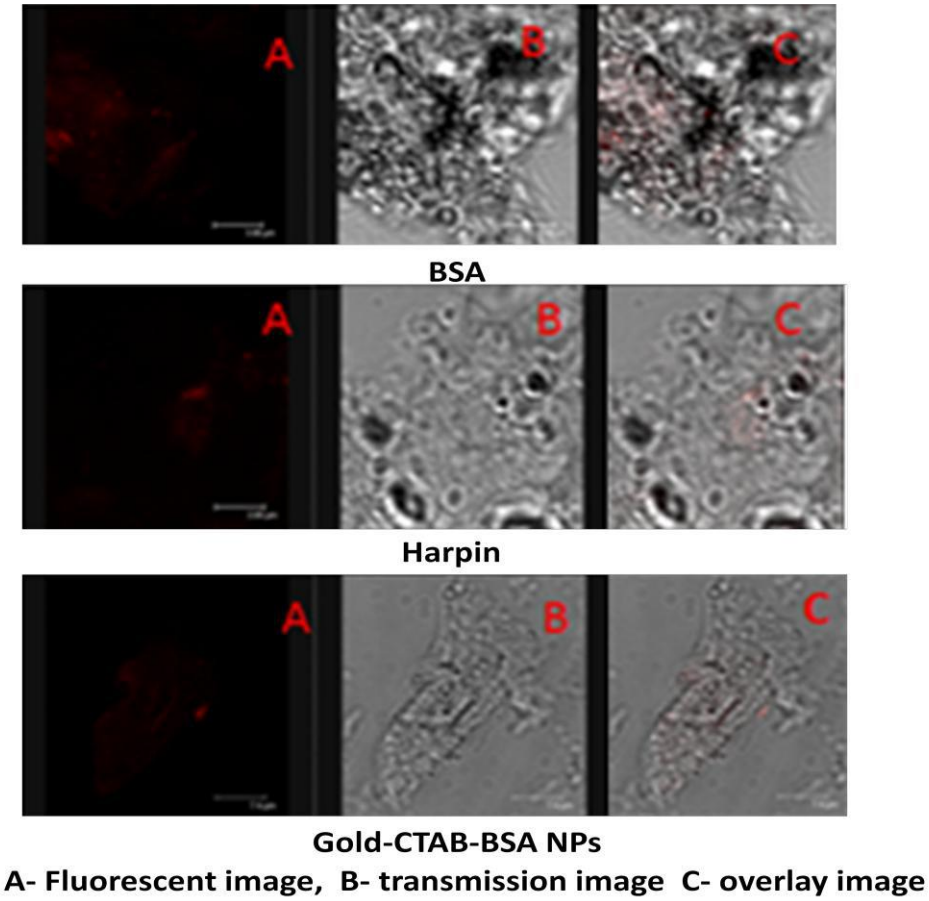

Figure 3.14.1: Confocal imaging of nanoparticles: Confocal images of BSA, Harpin, Gold-CTAB- BSA NPs. Harpin and BSA are labled with Rhodamine isothio cyanate. The proteins were bioconjugated to the nanoparticles and sprayed on the tobacco plant. The ultra thin sections of leaf were made with cryocut and observed under confocal microscope. . A is the fluorescent image, B is the transmission image, C is the superimposed images of the nanoparticles.

The gold-BSA and gold-CTAB-Harpin nanoparticles shows a clear fluorescent images and the overlay image also contains red coloured fluorescence indicating that nanoparticles are bioconjugated with RITC. Before the observation the nanoparticles were topically applied on the leaf and ultra thin sections were made with cryostat and observed under confocal microscope.

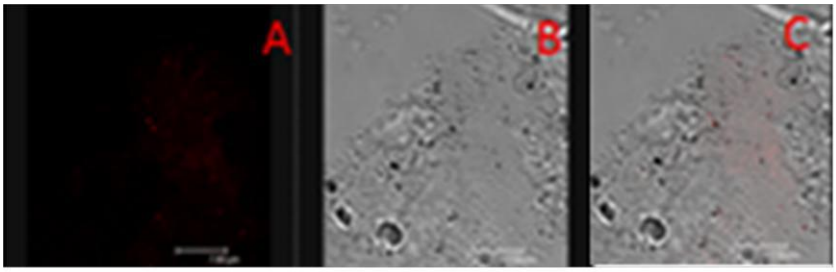

Gold BSA NPs

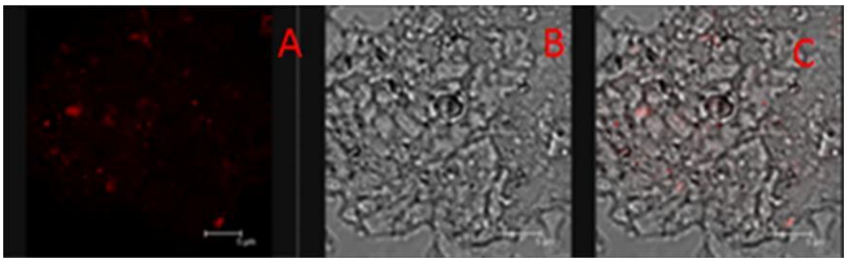

Gold-CTAB-Harpin Nanoparticles

A- Fluorescent image, B- transmission image C- overlay image

Figure 3.14.2: Confocal imaging of nanoparticles: Confocal image of Gold-BSA and Gold-CTAB Harpin NPs. Harpin was labled with Rhodamine isothio cyanate. The protein is bioconjugated to the nanoparticles and sprayed on the tobacco plant. The ultra thin sections of leaf were made with cryocut and observed under confocal microscope. A is the fluorescent image, B is the transmission image, C is the superimposed images of the nanoparticles.

3.15. Immunogold labelling of harpin

Tobacco plants were treated with gold nanoparticles and after 6 hrs of post treatment the sprayed regions were removed and immunogold labelling was done as per the methodology and observed under transmission electron microscope for localization. Particles were observed in and around the vacuole, cytoplasm, apoplast, cellwall and chloroplast which clearly informs that nanoparticles were internalized and they are distributed inside the plant cells. The nanoparticles which were sprayed were 13nm in size.

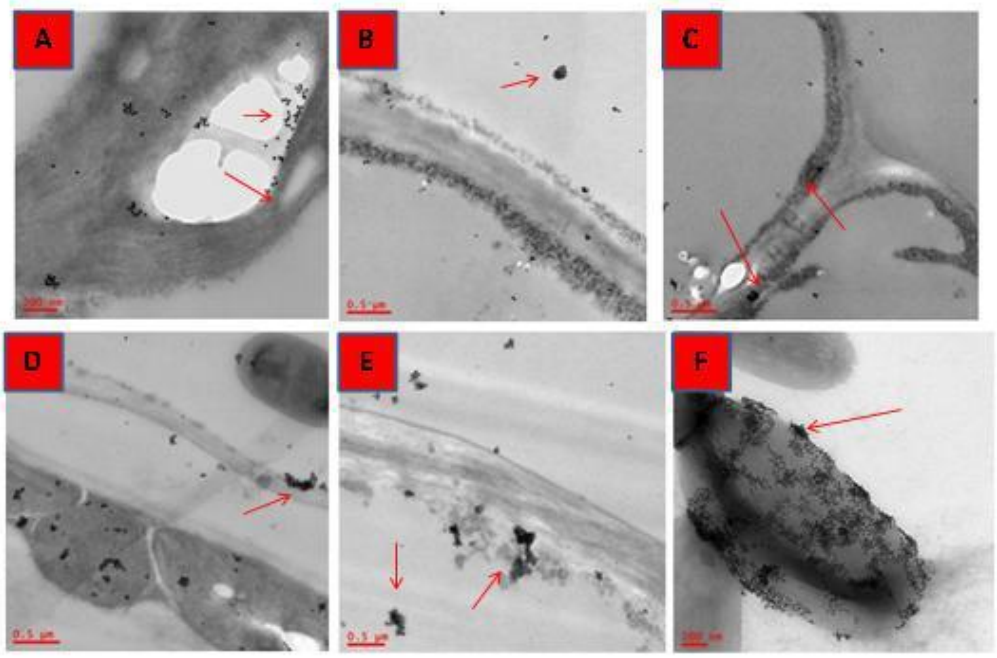

Figure 3.15: Immunogold labelling of harpin biofunctionalized nanoparticles. The localization of nanoparticles inside the plant cell are moving away from distant places through cytoplasmic connections. Then internalized nanoparticles were detected and present at different locations (A – in and around the vacuole; B – Cytoplasm; C- apoplast/on the cell wall; D- on the cell wall; E- Cytoplasm; F- Chloroplast) indicating that nanoparticles are entering from the epidermal openings and from their they are located to far distant places.

Discussion

4.1. Harpin – Elicitor protein involved in PCD of Plants

Harpins are hydrophilic, leucine & glycine-rich proteins that induce hypersensitive cell death in non host plants. They are dissimilar in amino acid sequence to each other and lack homology to any protein in the data base, thus making this class of proteins as the most potent and functionally challenging biological molecules on the earth (Kondreddy. 2011). Harpins seem to signal plants activating basal defense pathways and therefore can be used for topical application on plants to induce HR (Peng et al. 2004). Unlike chemical pesticides, it induces systemic resistance to the plant against wide variety of pathogens and insects without hampering the ecological balance. Being an ecofriendly molecule and its potentiality to induce resistance in wide variety of plants, harpin(s) is being used as a registered bio-pesticide or enhanced fertilizer (Plant Health Care : EDEN Biosciences). The capacity of inducing defense responses even at low concentrations of harpin depends on the retention time or extent of penetration of the protein into the extracellular spaces of the leaf surface which is facilitated by the molecules to which the protein is conjugated. In the present study we have chosen a proven biological elicitor molecule harpin as foliar spray for induction of disease resistance in tobacco. This is a maiden approach to deliver harpin in a nanoparticles form, in conjugation with chitosan for a topical spray.

4.2. Physico-Chemical characterization of Nanoparticles

Characterization and analysis of proteins entrapped into the chitosan is the crucial step for better understanding the nature of harpin loaded chitosan affects on biological samples. A comprehensive physico-chemical analysis which includes characterization of

synthesized nanoparticles will allow us to study the interaction of nanoparticles with the biological systems (Liu et al.2013).

The chitosan nanoparticles are synthesized by ionotropic gelation method.The positive charges on the chitosan combines with oppositely charged TPP. The ionization degree of TPP is determined by the pH value of the solution which inturn influences the surface morphology of nanoparticles and size (Ko et al. 2002)

.The size, surface morphology of observed nanoparticles in the current study correlates with several other nanoparticles studies of chitosan nanoparticles (Nadirah et al. 2014). The atomic force microscopic studies on synthesized nanoparticles revealed spherical shape for the both chitosan nanoparticles and harpin loaded chitosan nanoparticles which is in agreement with the results of scanning electron microscopic and as observed in other studies (Nadirah et al. 2014).

The surface charge property of a nanoparticles is studied by zeta potential. It indicates the electric potential of particles in the solution in which it is present. In the current study, the zeta potential of nanoparticles revealed negative charge for the citrate capped gold nanoparticles and positive for the gold CTAB particles as observed in other studies. Nanoparticles which posses a zeta potential above 30 m V (+/-) are known to be constant in solution because of the surface potential which prevents aggregation of the particles. Zeta potential is also used to measure a compound is encapsulated or adsorbed on the surface.

4.3. Harpin nanoparticles for induced defense response

Harpin protein solution (20µg/ml) was sufficient to induce HR when infiltrated on tobacco leaves as observed in other studies (Dong et al. 2004 : Wu et al. 2008). Harpin-loaded Chitosan nanoparticles at much lower concentration of harpin (30ng/ml) showed the HR which coincided with the expression of defense related genes *hin, hsr, chia-5*.(Wu at al. 2008) reported inducible expression of *PR-1a* and *PR-1b* in tobacco plants when treated with HpaG. The application of harpin-loaded CS-NPs will be a good choice for improving defense system in plants, due to slow release rate of protein which facilitates longer retention on leaf surface. The immediate release of the protein from the particle was very less as it was in the core with strong electrostatic interactions between harpin and CS, which possibly contributed to the slow release of harpin from the harpin-loaded CS-NPs. The releasing kinetics of harpin from harpin loaded CS-NPs shows 33% release in the first 30 minutes and reached to 57% in the next 60 minutes. There after no release of harpin was observed even after 24 hours.

4.4. Generation of ROI during HR

Quick production of reactive oxygen species (ROS) is the key components generated in elicitor mediated HR (Lu et al. 1998). Accumulation of ROS at the site of spray correlated with the fluorescence in the current results. Extensive fluorescence was observed with the harpin-loaded CS-NPs sprayed region than the chitosan, TPP or harpin-treated leaves (Figure 3.12) indicating that the ROS indeed accumulated in the CS-NPs-treated region and not with other treatments as observed with ROS studies using harpin as elicitor.

4.5. PCD and Callose Deposition during HR

Plants challenged with pathogens or elicitors often show signs of programmed cell death (PCD) in the form of nuclear condensation which can be visualized by DAPI staining. Nuclear condensation in *Nicotiana tabacum* suspension cells treated with PB90, a protein elicitor secreted by *Phytophthora boehmeriae* that induces HR in tobacco plants (Kondreddy 2013). Similarly tobacco plants treated with harpin-loaded CS NPs showed condensed nuclei as bright spots compared to the plants treated with TPP, harpin, chitosan and water suggesting the signs of PCD around the region of nanoparticle treatment.

Defense reactions initiated by the plant are usually multi-component and complex but often occur as a rapid localized cell death at the region of infection to contain the pathogen, as well as a systemic acquired resistance throughout the plant (Govrine and Levine. 2000). The *hin and hsr* are considered as marker genes in the hypersensitive cell death (Lee et al. 2001) whereas the *Chia-5* is a defense related gene involved in salicylic acid-induced defense pathway (Peng et al. 2004). The induced expression of *hin, hsr, chia-5* was in the harpin-loaded CS-NPs treated leaves, which is consistent with the micro HR, compared to the harpin and chitosan-treated leaves. We have analyzed the distance at which the CS-NPs induced defense-related changes would occur as also the fate of these nanoparticles in the treated plants.

Nanoencapsulation of harpin would also induce defense responses like callose accumulation, lipid peroxidation because of better penetration through tissues and allowing a slow and constant release. Callose deposition gives resistance to *Erisiphe*

graminis f.sp.hordei and deposition of callose was observed at the haustoria of downy mildew and powdery mildew, rust fungi (Gorg et al.1993). However accumulation of callose does not act as an effective resistance towards rust infections. The presence of more amount of callose after 6h of application represents a rapid and quicker HR in and around the site of CS-NP region whereas few areas of callose deposition were found in other treatments.

4.6 Induction of HR by gold nanoparticles.

In the preparation of gold nanoparticles two types of methods are employed. Citarate and CTAB surface capped gold nanoparticles. In the preparation of negatively chargrd citrate capped gold nanoparticles tetrachloroauric acid was reduced by sodium citrate. Tetrachloroauric caid was heated to high temperature and trisodium citrate was mixed to them resulting in the formation of monodisperse Au NP (gold nanoparticles through nucleation process and successively to form Au NPs. These gold nanoparticles later surface coated by the citrate ions of the sodium citrate giving negative charge to the particles. The citrate capped Au NPs were can be attached with proteins. The attachment of protein molecules occurs through electrostatic interactions. The lysine parts of the protein which are positively charged adsorbed to negatively charged citate on the nanoparticles. The isoelectric points of BSA is between 4.5 and 4.9 and harpin 4.2 therefore in the Millipore water at a value of pH 7 the BSA and Harpin which contains high number of negative charges forms couloumbic force of attaraction among the protein molecules and citrate capped AuNPs. The CTAB encapsulated AuNPs imparted with positive interfacial surface charge. Sodiumborohydrate, stabilizes the gold surface to which the cationic CTAB head groups surround by electrostatic interactions pointing out

the hydrophobic tail with positive interfacial charge. Harpin and BSA suspended in the solution which renders them negative charge, giving scope for the formation of electrostatic interactions by which proteins were conjugated to the CTAB encapsulated AuNPs. Ionic, hydrogen bonding is also possible apart from electrostatic interactions. The binding energies for such bonds are 10-30 kcal/mol. So lysine rich proteins like BSA and harpin are highly attractive towards these nanoparticles (Wangoo *et al* 2008). The Transmission Electron Micrographs of the citrate capped AuNPs with negative charge and CTAB encapsulated AuNPS by positive interfacial charge visualized increased in the size of bioconjugated protein AuNPs.

Size, shape controlled nanoparticles in aqueous solution could be studied by UV-visible spectroscopy. Different amounts of the protein conjugated to nanoparticles starting from 10 to 70 µg/ml were studued with UV-visible spectrophotometer. The absorption spectra of the harpin conjugated nanoparticles manifests presence of increasing sharp peaks as the concentration of the conjugated protein increased. The broadening and red shift in the peak represents the formation of bioconjugates. The position of the maximum absorption shifted from 520 nm to 523 nm for harpin AuNPs, 523 for BSA AuNPs where as CTAB encapsulated AuNPs showed 530 nm. The UV-visible spectrophotometric analysis of BSA and harpin conjugated nanoparticles found stable.

5.5. Molecular detection of HR induced defense genes upon treatment with nanoparticles

The foliar application of AuNPs resulted in the accumulation of pathogen related gene transcripts like *Chia-5, hin, PR-1* and *PR-2,*. RT-PCR in the case of citrate capped AuNPs, control , gold conjugated BSA treated plants not induced any of the gene

transcripts. Harpin application on tobacco plants induced basal level expression of *PR-1* and *PR-2* . The strong amplification of *PR-1, PR-2, Chia-5* and *hin* was observed in the harpin bioconjugated citrate capped AuNPs. The harpin conjugated CTAB encapsulated AuNPs activated dense expression of *hsr, hin, Chia-5, PR-1, PR-2,* and *PR-3*. indicating the hypersensitive response at the molecular level.

In plant- pathogen interactions elicitors produced by the pathogen induce defense which involve the production of phytoalexins, synthesis of defense related proteins. *PR-1* known to be active against oomycetes and often considered as the marker for systemic acquired resistance. The *PR-2* proteins comes under the family β – 1,3-endoglucanases and *PR-3* considered as endochitinases which are effective against fungi and also limit growth and spread pathogen activity. The *chia-5* could work on nematodes and herbivorous insects (Van Loon et al 2006). Harpin protein solution (20 µg/mL) was sufficient to induce HR when infiltrated on tobacco leaves (Dong *et al*., 2004). Harpin-bioconjugated AuNPs as a foliar spray (70 ug/mL) showed the expression of defense related genes *hin, hsr, chia-5, PR-1, PR-2, PR-3.* The application of harpin- conjugated AuNPs will be a good choice for improving defense system in plants, due to bioavailability of protein which facilitates longer retention on leaf surface.

Defense reactions initiated by the plant are usually multi-component and complex but often occur as a rapid localized cell death at the region of infection to contain the pathogen, as well as a systemic acquired resistance throughout the plant (Govrine and Levine, 2000). The *hin and hsr* are considered as marker genes in the hypersensitive cell death (Lee et al. 2001) whereas the *Chia-5* is a defense related gene involved in salicylic acid-induced defense pathway. The induced expression of *hin, hsr, chia-5, PR-1, PR-2,*

PR3 consistent with the micro HR, compared to the harpin conjugated AuNPs . We also analyzed the distance at which the AuNPs induced defense-related changes would occur as also the fate of these nanoparticles in the treated plants.

The efficiency of delivery of bioconjugated harpin into plant cells was monitored by RITC conjugated nanoparticles. The RITC conjugated nanoparticles sprayed on the leaf of the plant and observed after 6h of foliar application. The leaf sample was sectioned using cryostat (LEICA CM 1850 UV) and observed under confocal microscope (LEICA Laser scanning confocal microscope TCS SP2 AOBS Germany). The fluorescent nanoparticles were evident in the vicinity of stomata and were located to distant regions from the epidermal openings which can be visualized as red coloured dots in the intercellular spaces apoplastic regions in the chloroplast and inside the cells. This clearly indicates that the bioconjugated fluorescent labelled nanoparticles were moving inside the cell through cell to cell connections and prominent in the apoplastic regions. The presence of fluorescence detected in the in and around of stomata suggesting that the these openings are the locations for the entry of nanoparticles where as some of them rupture the surface as they were denser .The presence of these fluorescent particles all through the section opining that they were slowly moving to distant locations from where they were applied enabling the bioavailability of harpin for longer duration of time. This temporal movement will give chance to the particles to spread and to show a quicker HR than the infiltration. However, this method of application is cost effective and less labour intensive.

Earlier, the immunogold labelling methodology was purely employed for immunohistochemical studies. However, in the recent past, imunogoldlabelling method

has become an important technique for detecting the penetration of nanoparticles In the immunogold labelling of harpin gold nanoparticles of 13nm in size were sprayed on the plant. After 6 hours of post treatment leaf sections were subjected to the methodology of immunogold labelling and observed the presence of gold nanoparticles inside the plant. They were got accumulated in the cytoplasm, apoplast, cell wall and in and around the vacuole giving an evidence that these nanoparticles were localized and they are moving inside the plant cells from cell to cell connections. This examination clearly manifests the presence of gold nanoparticles inside the cellular environment.

Major findings

The work undertaken in the thesis is presented with the following major findings:

1. Synthesized and Characterized Harpin Loaded Chitosan Nanoparticles which can induce defense responses in tobacco.
2. The synthesized Harpin Loaded Chitosan Nanoparticles and Gold Nanoparticles are characterized using Transmission Electron Microscope, Scanning Electron Microscope, Atomic Force Microscopy and confirmed physico-chemical properties of nanoparticles.
3. Defense-related genes (*hin, hsr, chia-5; PR-1; PR-2 and PR-3*) showed induced expression in tobacco leafs treated with various nanoparticles.
4. Histochemical analysis (Reactive Oxygen Intermediates, Callose Deposition, Nuclear Condensation Studies) revealed induced defense responses with harpin loaded chitosan nanoparticles .
5. Localization studies using RITC method revealed successful penetration of gold nanoparticles into various cellular compartments.

Summary and Conclusions

Summary:

Biopolymeric nanoparticles like chitosan nanoparticles and metallic nanoparticles like gold nanoparticles with citrate and CTAB capped negative and positive surface charge containing nanoparticles were prepared. Physico chemical characterizations of these nanoparticles were done with Transmission electron microscope (TEM), Atomic force microscope (AFM) and scanning electron microscope (SEM). The chitosan nanoparticles were characterized by SEM and AFM, and are found to be spherical in shape and almost equal in size. The nanoparticles were found to possess smooth surfaces with harpin entrapped into them. The releasing kinetics revealed that the loaded harpin was released up to 60 minutes. The association efficiency and loading capacity were calculated. The nanoparticles which were loaded with harpin when sprayed on the plant showed defense response like callose deposition, generation of reactive oxygen intermediates and nuclear condensation. The molecular assays like RT-PCR showed induced expression of defense related genes *like hsr, hin and chia-5.*

The gold nano particles with citrate capped are negatively charged and possess negative zeta potentials and CTAB capped nanoparticles are positively charged with positive interfacial surface charge. These nanoparticles were utilized for the topical application on the tobacco plant. These particles are having very small size (13 nm) and well dispersed from each other. The flocculation studies were conducted for citrate capped gold nanoparticles to observe the surface stabilization. The protein concentration of 70 µg/ml showed stable citrate capped gold nanoparticles. The UV-visible characterization of these nanoparticles added with 10% NaCl showed similar results with flocculation assay. The

UV-visible characterization of gold CTAB, gold Harpin, gold BSA showed 50 µg/ml and 40 µg/ml are sufficient for surface sterilization of these nanoparticles. The zeta potentials of citrate capped possess negative zeta potentials and CTAB capped possess positive zeta potentials. The nanoparticles adsorbed with Harpin when applied on the leaf of the tobacco leaves showed induced expression of *PR-1, PR-2, PR-3 chia-5, hsr, hin* transcript levels, when treated with gold and its conjugates. Localization studies conducted with RITC conjugated nanoparticles showed showed fluorescence in the ultra thin sections, indicating that the topically applied RITC conjugated nanoparticles are present inside the plant cells which entered through epidermal openings and their onwards moving inside the plant through cell to cell connections. The immunogold labelling studies revealed the presence of nanoparticles in and around the vacuole, cytoplasm, apoplast, and cell wall indicating that nanoparticles were localized and present inside the cells and moving away from the site of entry.

Conclusions:

The harpin loaded nanoparticles were large in size when compared with the gold and its conjugates. The gold nanoparticles are having more penetrating capacity than the chitosan nanoparticles. The concentration of 30 ng/ml which were loaded on to chitosan nanoparticles showed induced defense responses in the plant. Because of their small size gold nanoparticles expressed a strong amplification of defense related genes than the chitosan nanoparticles. A gold nanoparticle can be stored at 4^0C in dark for six months so, the availability of gold nanoparticles is easier than the chitosan nanoparticles. The chitosan nanoparticles are biocompatible, degradable with positive surface charge but the

gold nanoparticles possess toxic effects on the human being. The chitosan nanoparticles release the protein very slowly which induces histochemical reactions in the plant cells. Further, chitosan nanoparticles and gold nanoparticles showed micro HR in the plant cells. The UV-Visible characterization, silver staining effectively showed that the proteins are adsorbed on the nanoparticles surface.

The gold nanoparticles conjugated with RITC showed presence of these nanoparticles inside the plant cells and immunogold labelling of harpin also showed the treated gold nanoparticles localized in different regions of plant cells indicating that topically applied gold nanoparticles have entered into the plant cells.

References

References:

Adam JL and Somerville SC (1996) Genetic characterization of five powdery mildew disease resistance loci in *Arabidopsis thaliana,* The Plant Journal 9(3):341-356.

Agnihotri SA, Mallikarjuna NN, Aminabhavi TM (2004) Recent advances on chitosan-based micro- and nanoparticles in drug delivery, Journal of Controlled Release 100: 5-28.

Aguilar Mendez M, San Martin ME, Ortega AL, Cobin PG, Snchez EE (2011) Synthesis and characterization of silver nanoparticles: effect on phytopathogen *Colletotrichum gloesporioides*. J Nanoparticle Res 13:2525-2532.

Artursson P, Lindmark T, Davis SS, Illum L (1994) Effect of chitosan on the permeability of monolayer of intestinal epithelial cells (Caco-2). Pharm Res11:1358–1361.

Aspden TJ, Mason JD, Jones NS (1997) Chitosan as a nasal delivery system: the effect of chitosan solutions on in vitro and in vivo mucociliary transport rates in human turbinates and volunteers. J Pharm Sci 86:509-513.

Baier AC (2009) Regulating nanosilver as a pesticide. Environmental Defense Fund, February 12.

Baneyx G, Baugh L, Vogel V (2001) Coexisting conformations of fibronectin in cell culture imaged using fluorescence resonance energy transfer. Proc Nat Acad Sci USA 98:14464- 14468.

Berthold A, Cremer K, Kreuter J (1996) Preparation and characterization of chitosan microspheres as drug carrier for prednisolone sodium phosphate as model for anti inflammatory drugs. J Control Release 39:17–25.

Borkow G and Gabbay J (2005) Copper as a biocidal tool. Curr Med Chem 12(18):2163-2175.

Bradford MM (1976) A rapid and sensitive for the quantitation of microgram quantitites of protein utilizing the principle of protein-dye binding. Anal Biochem 72: 248-254.

Brecht M Datnoff L, Nagata R, Kucharek T (2003) The role of silicon in suppressing tray leaf spot development in St.Augustine grass. Publication in University of Florida, 1-4.

Bruchez M, Moronne M, Gin P, Weiss S, Alivisatos AP (1998) Semiconductornanocrystals as fluorescent biological labels. Science 281:2013-2016.

Brunel F, El Gueddari NE, Moerschbacher BM (2013) Complexation of copper(II) with chitosan nanogels: toward control of microbial growth. Carbohydr Polym 15-92(2):1348-1356.

Calvo P, Remun C, Vila JJL, Alonso MJ (1997) Novel hydrophilic chitosan-polyethylene oxide nanoparticlesas protein carriers. J Appl Polym Sci 63:125-132.

Carver TLW, Thomas BJ, Robbins MP, Zeyen RJ (1998). Phenylalanine ammonia-lyas e inhibition, autofluorescence, and localized accumulation of silicon, calcium and manganese in oat epidermis attacked by the powdery mildew fungus *Blumeria graminis* (DC) Speer. Phy Mol Plant Pathol 52: 23-243.

Chookhongkha N, Miyagawa S, Jirakiattikul Y, Photchanachai S (2012) Chili growth and seed productivity as affected by chitosan. International Conference on Agriculture Technology and Food Sciences (ICATFS'2012) Nov. 17-18, 2012 Manila, Philippines.

Clement JL and Jarrett PS (1994) Antibacterial silver. Metal Based Drugs1:467-482.

Couzin J (2002) Breakthrough of the year: Small RNAs make big splash. Science 20:298(5602):2296-2297.

Davis AV, Yeh RM, Raymond KN (2002) Supramolecular assembly dynamics. Proc Natl Acad Sci USA 99:4793-4796.

Derk JM R, Wang L, Godleski J, Kobzik L, Brain J, Demokritou P (2014) Tracking translocation of industrially relevant engineered nanomaterials (ENMs) across alveolar epithelial monolayers in vitro. Nanotoxicology 1:216-225.

Dong HP, Peng JL, Bao ZL, Meng XD, Bonasera JM, Chen GY, Beer SV, Dong HS (2004) Downstream divergence of the ethylene signalling pathway for harpin-stimulated *Arabdiopsis* growth and insect defense. Plant Physiol 36:3628-3638.

Dubertret B, Skourides P, Norris DJ, Noireaux V, Brivanlou AH, Libchaber A (2002) In vivo imaging of quantum dots encapsulated in phospholipid micelles. Science 29(298):1759 1762.

Dumitriu S and Esteban Chornet E (1998) Inclusion and release of proteins from polysaccharide-based polyion complexes. Adv Drug Delivery Rev 31(3):223-246.

Edelstein RL, Tamanaha CR, Sheehan PE, Miller MM, Baselt DR, Whitman LJ, Colton RJ (2000)The BARC biosensor applied to the detection of biological warfare agents. Biosensors Bioelectron14:805-813.

EDEN biosciences http://www.planthealthcare.com/technology/harpin/

Jain N,Bhargava A, Majumdar S, Tarafdar JC and Panwar J (2010) Extracellular biosynthesis and characterization of silver nanoparticles using *Aspergillus flavus* NJP08: A mechanism perspective

Felt O, Buri P, Gurny R (1998) Chitosan: A unique polysaccharide for drug delivery. Drug Dev. Ind. Pharm. 24: 979-993.

Fox RF and Choi MH (2001) Rectified Brownian motion of kinesin motion along microtubules. Phys Rev E Stat Nonlin Soft Matter Phys. 63:051901.

Frens G (1973) Controlled Nucleation for the Regulation of the Particle Size in Monodisperse Gold Suspensions. Nature Phys Sci 241:20– 22.

Gan L, XuWY, Jiang MS, He BH, SuMJ (2010). A Study on the Inhibitory Activities of Nano-silver to *Xanthomonas.campest ris* pv. campest ris. ActaAgriculturae Universitatis Jiangxiensis, 3:16.

Garcia-Rincun J, Vega-Purez J, Guerra-Snchez MG, Hernndez-Lauzardo AN, Peoa-Diaz A, Velzquez DVMG (2010). Effect of chitosan on growth and plasma membrane properties of *Rhizopus stolonifer* (Ehrenb.:Fr.) Vuill. Pest Biochem Phys 97:275-278.

Gorg R, Hollricher K, Schulze PL (1993) Functional analysis and RFLP – mediated mapping of the *MIg* resistance locus in barley. The Plant Journal 3(6):857-866.

Govrin EM, Levine A (2000) The hypersensitive response facilitates plant infection by the necrotrophic pathogen *Botrytis cinerea*, Current Biology10: 751-757.

He L, Liu Y, Mustapha A, Lin M (2011) Antifungal activity of zinc oxide nanoparticles against Botrytis cinerea and *Penicillium expansum*. Microbiol Research, 166: 207-215.

He, SY, Huang, HC & Collmer, A (1993). *Pseudomonas syringae pv. syringae* harpin$_{SS}$: a protein that is secreted via the Hrp pathway and elicits the hypersensitive response in plants. Cell 73:1255-1266.

Ikai A, Idiris A, Sekiguchi H, Arakawa H, Nishida S (2002) Intra- and intermolecular mechanics of proteins and polypeptides studies by AFM. Appl Surf Sci 188:506-512.

Illum L, JabbalGI, Hinchcliffe M, Fisher AN, Davis SS (2001) Chitosan as a novel nasal delivery system for vaccines. Adv. Drug Deliv. Rev. 51: 81-96.

Jain D and Banerjee R (2008) Comparison of ciprofloxacin hydrochloride-loaded protein, lipid, and chitosan nanoparticles for drug delivery. J Biomed Mater Res 86:105–112.

Janes KA, Calvo P, Alonso MJ (2001) Polysaccharide colloidal particles as delivery systems for macromolecules. Adv Drug Deliv Rev 47:83–97.

Jo YK, Kim BH, Jung G (2009) Antifungal activity of silver ions and nanoparticles on phytopathogenic fungi. Plant Disease 93:1037-1043.

Joseph A, Itskovitz CN, Samira S, Flasterstein O, Eliyahu H, Simberg D, Kedar E (2006) A new intranasal influenza vaccine based on a novel polycationic lipid - ceramide carbamoyl spermine (CCS): I. Immunogenicity and efficacy studies in mice. Vaccine, 24(18): 3990-4006

Kashyap PL, Xiang X, Heiden P (2015) Chitosan nanoparticle based delivery systems for sustainable agriculture. Int J Biol Macromolecules 77:36-51.

Khodakovskaya M V, de Silva K, BirisAS, Dervish E, Villagarcia H (2012) Carbon nanotubes induce growth enhancement of tobacco cells. ACS Nano 6:2128-2135.

Khodakovskaya M, Dervishi E, Mahmood M, Xu Y, Li Z, Watanabe F, Biris AS (2009) Carbon nanotubes are able to penetrate plant seed coat and dramatically affect seed germination and plant growth. ACS Nano 3:3221-3227.

Kolhe P and Kannan RM (2003) Improvement in ductility of chitosan through blending and copolymerization with PEG: FTIR investigation of molecular interactions. Biomacromolecules 4(1):173-180.

Ko JA, Park, HJ, Hwang SJ Park, JB & Lee, JS (2002) Preparation and characterization of chitosan microparticles intended for controlled drug delivery. International Journal of Pharmaceutics 249:165–174

Kondreddy A (2011) Elicitor-mediated defence responses in ground and tobacco, Phd Thesis, University of Hyderabad.

Kondreddy Anil, Subha Narayan Das Appa Rao P (2014) Induced Defense in Plants: A Short Overview. Proc Natl Acad Sci, India, Sect B Biol Sci 84(3):669–679.

Kong M, Chen XG, Xing K, Park HJ (2010) Antimicrobial properties of chitosan and modeof action:a state of the art review. Int J Food Microbiol 144: 51-63.

Lamsal K, Kim SW, Jung JH, Kim YS, Kim KS, Lee YS (2011a) Application of silver nanoparticles for the control of *Colletotrichum* species *In vitro* and pepper anthracnose disease in field. Mycobiology 39:194-199.

Lamsal K, Kim SW, Jung JH, Kim YS, Kim KS, Lee YS (2011b). Inhibition effects of silver nanoparticles against powdery mildews on cucumber and pumpkin. Mycobiology 39:26-32.

Lee J, Klessig DF, Nürnberger T (2001) A harpin binding site in tobacco plasma membranes mediates activation of the pathogenesis-related gene HIN1 independent of extracellular calcium but dependent on mitogen-activated protein kinase activity.Plant Cell13(5):1079 1093.

Li J, Yun H, Gong Y, Zhao N, Zhang X (2006) Investigation of MC3T3-E1 cell behavior on the surface of GRGDS-coupled chitosan. Biomacromolecules 7(4):1112-1123.

Liu H, Yang D, Yang H, Zhang H, Zhang W, Fang Y, Lin Z, Tian L, Lin B, Yan J, Xi Z (2013) Comparative study of respiratory tract immune toxicity induced by three sterilisation nanoparticles: silver, zinc oxide and titanium dioxide. J Hazard Mater. Mar 15; 248-249:478-86.

Lower SK, Hochella MFH, Beveridge TJ (2001) Bacterial recognition of mineral surfaces: nanoscale interactions between Shewanella and a-FEOOH. Science292:1360-1363.

Lu H, Higgins VJ (1998) Measurementof active oxygen species generated in Planta in response to elicitor AVR9 of *Cladosporium fulvum*. Physiol Mol Plant Path 52:35-51.

Madihally SV and Matthew HWT (1999) Porous chitosan scaffolds for tissue engineering. Biomaterials. 20:1133–1142.

Mah C, Zolotukhin I, Fraites TJ, Dobson J, Batich C, Byrne BJ (2000) Microsphere-mediated delivery of recombinant AAV vectors *invitro* and *in vivo*. Mol Therapy1:S239.

Mahmoodzadeh H, NabaviM, KashefiH (2013) Effect of nanoscale titanium dioxide part icles on the germination and growth of canola (*Brassica napus*). J Ornamental and Horticultural Plants 3:25-32.

Mazzola L (2003) Commercializing nanotechnology. Nat Biotechnol 21:1137-1143.

Mishra S, Keswani C, Abhilesh PC, Leonardo FF and Singh HB (2017) Integrated approaches of agri-nanotechnology : Challenges and future trends. Frontiers in Plant Science 8:471.

Min JS, Kim KS, Kim SW, Jung JH, Lamsal K, KimSB, Jung M, Lee YS (2009) Effects of colloidal silver nanoparticles on sclerotium-formingphytopathogenic fungi. Journal of Plant Pathology 25:376-380.

Misevic GN (2001) Atomic force microscopy measurements: binding strength between a single pair of molecules in physiological solutions. Mol Biotechnol 18:149-154.

Mondal K and Mani C (2012) Investigation of the antibacterial properties of nanocopper against *Xanthomonas axonopodis* pv. *punicae*, the incitant of pomegranate bacterial blight. Annals of Microbiology 62:889-893.

Nadirah ABR, Chin SF, Pang SC, Bilung LM (2014) Preparation and characterization of Chitosan Nanoparticles-doped cellulose films with antimicrobial property. Journal of Nanomaterials .10.

Nasongkla N, Bey E, Ren JM, Ai H, Khemtong C, Guthi JS, Chin SF, Sherry AD, Boothman DA, Gao JM (2006) Multifunctional polymeric micelles as cancer-targeted, MRI ultrasensitive drug delivery systems. Nano Lett 6(11):2427–2430.

Panatarotto D, Prtidos CD, Hoebeke J, Brown F, Kramer E, Briand JP,Muller S, Prato M, Bianco A (2003) Immunization with peptide-functionalizedcarbon nanotubes enhances virus specific neutralizingantibody responses. Chemistry and Biology10:961-966.

Park HJ, Kim SH, Kim HJ, Choi SH (2006) A New composition of nanosized silica-silver for control of various plant diseases. Journal of Plant Pathology22: 295-302.

Paull R, Wolfe J, Hebert P, Sinkula M (2003) Investing in nanotechnology. Nat Biotechnol 21, 1144-1147.

Peng J, Dong H, Delaney TP, Bonasera JM, Beer SV (2003) Hrpin- elicited hypersensitive cell death and pathogen resistance require the *NDR1* and *EDS1* genes. Physiol Mol Plant Pathol 62: 317-326.

Peng JL, Bao ZL, Ren HY, Wang JS, DongHS (2004) Expression of $Harpin_{xoo}$in transgenic tobacco induces pathogen defense in the absence of hypersensitive cell death, Phytopathology. 94:1048-1053.

Pinto RJ, Almeida A, Fernandes SC, Freire CS, Silvestre AJ, NetoCP, Trindade T (2013) Antifungal activity of transparent nanocomposite thin films of pullulan and silver against *Aspergillus niger*. Colloids and Surfaces B: Biointerfaces103:143-148.

Prasad T NVKV, Sudhakar P, Sreenivasulu Y, Latha P, Munaswamy V, Reddy KR, Sreeprasad TS,Sajanlal PR, Pradeep T (2012) Effect of nanoscale zinc oxide particles on the germination, growth and yield of peanut. J Plant Nutrition 35: 905-927.

Prasun P and Goswami A (2012) Zinc nitrate derived nano ZnO: Fungicide for disease management of horticultural crops. Int J Innov Horticulture 1:79-84.

Prins A, Van Heerden PD, Olmos E, Kunert KJ, Foyer CH (2008) Cysteine proteinases regulate chloroplast protein content and composition in tobacco leaves: a model for dynamic interactions with ribulose-1,5-bisphosphate carboxylase/oxygenase (Rubisco) vesicular bodies. J Exp Bot 59(7):1935-1950.

Qi LF, Xu ZR, Jiang X, Hu CH, Zou XF (2004) Preparation and antibacterial activity of chitosan nanoparticles. Carbohydrate Research 339:2693–2700.

Qi LF, Xu ZR, Jiang XY, Wang MQ (2005) Cytotoxic activities ofchitosan nanoparticles and copper-loaded nanoparticles. Bioorganic and Medicinal Chemistry Letters 15:1397-1399.

Qi, LF, & Xu, Z. R (2004) Lead sorption from aqueous solutions on chitosan nanoparticles. Colloids Surfaces A: Physicochemical Engineering Aspects, 251:183–190.

Qi, L & Xu, Z (2006) In vivo antitumor activity of chitosan nanoparticles. Bioorganic & Medicinal Chemistry Letters, 16(16), 4243-4245.

Qian K, Shi T, Tang T, Zhang S, Liu X, Cao Y (2011) Preparation and characterization of nano-sized calcium carbonate as controlled release pes ticide carrier for validamycin against *Rhizoctonia solani*. Microchimica Acta 173: 51-57.

Roller S and Covill N (1999) The antifungal propert ies of chitosan in laboratory media and apple juice. Int J Food Microbiol 47:67-77.

Sachlos E, Gotora D, Czernuszka JT (2006) Collagen Scaffolds Reinforced with biomimetic Composite Nano-Sized Carbonate-Substituted Hydroxyapatite Crystals and Shaped by Rapid Prototyping to Contain Internal Microchannels. Tissue Engineering 12(9):2479-2487.

Schipper NGM, Olsson S, Hoogstraate JA, de Boer AG, Vårum KM, Artursson P (1997) Chitosans as absorption enhancers for poorly absorbable drugs 2: mechanism of absorption enhancement. Pharm Res 14:923-929.

Schipper NGM, Vårum KM, Artursson P (1996) Chitosans as absorption enhancers for poorly absorbable drugs.1: influence of molecular weight and degree of acetylation on drug transport across human intestinal epithelial (Caco-2) cells. Pharm Res 13:1686-1691.

Schipper NGM, Vårum KM, Stenberg P, Ocklind G, Lennernäs H. Artursson P (1999) Chitosons as absorption enhancers of poorly absorbable drugs 3: influence of mucus on absorption enhancement. Eur J Pharm Sci 8: 335-343.

Shang L, Dorlich RM, Brandholt S, Schneider R, Trouillet V, Bruns M, Gerthsen D, Nienhaus GU (2011) Facile preparation of water-soluble fluorescent gold nanoclusters for cellular imaging applications. Nanoscale 3:2009–2014.

Sharma K, Sharma R, Shit S, Gupta S (2012) Nanotechnological application on diagnosis of a plant disease. Internat ional Conference on Advances inBiological and Medical Sciences (ICABMS.2012) .

Sripriya P, Vedantam LV, Podile AR (2009) Involvement of mitochondria and metacaspase elevation in harpin$_{PSS}$-induced cell death of *Saccharomyces cerevisiae.* J Cell Biochemistry 107:1150 – 1159.

Sudarshan NR, Hoover DG, KnorrD (1992) Antibacterial action of chitosan. Food Biotechnology 6:257-272.

Takeuchi H, Yamamoto H, Niwa T, Hino T, Kawashima Y(1996) Enteral absorption of insulin in rats from mucoadhesive chitosan-coated liposomes. Pharm Res 13: 896–901.

Tiwari NR, Rathore A, Prabhune A, Kulkarni SK (2010) Gold nanoparticles for colorimetric detection of hydrolysis of antibiotics by penicillin G acylase. Advances in Bioscience and Biotechnology 1: 422-329.

Torney F, Trewyn BG, Lin VSY, Wang K (2007) Mesoporous silica nanoparticles deliver DNA and chemicals into plants. Nature Nanotechnology 2:295-300.

USEPA (2007) Framework for Determining a Mutagenic Mode of Action for Carcinogenicity.Review Draft. EPA 120/R-07/002-A.

Van Loon LC, Rep M, Pieterse CMJ (2006) Significance of inducible defense-related proteins in infected plants. Ann Rev Phytopathol 44:135-162.

Vaseashta A. and Dimova-Malinovska D (2005) Nanostructured and nanoscale devices, sensors and detectors Sci Tech Adv Materials 6:3-4.

Waheed AA and Gupta PD (1999) Single-step method for estimating nanogram quantities of Protein. Anal Biochem 275(1):124-127.

Wang S, Mamedova N, Kotov NA, Chen W, Studer J (2002)Antigen/antibody immunocomplex from CdTe nanoparticlebioconjugates. Nano Letters 2:817-822.

Wangoo N, Bhasinb KK, Mehtab SK, Raman Suri C (2008) Synthesis and capping of water dispersed gold nanoparticles by an amino acid: Bioconjugation and binding studies. J Coll Interface Science 323(2):247-254.

Warren C, Chan W, Nie S (1998) Quantum dot bioconjugates for ultrasensitive nonisotopic detection. Science 281: 2016-2018.

Wei ZM, Laby, RJ, Zumoff, CH Bauer, DW, He, SY, Collmer, A & Beer, SV (1992) Harpin, elicitor of the hypersensitive response produced by the plant pathogen Erwinia amylovora. Science **257**: 85-88.

Wu H, Wang S, Qiao J, Liu J, Zhan J, Gao X (2008) Expression of *HpaG*$_{Xooc}$ protein in *Bacillus subtilis* and its biological functions. J Microbial Biotecnol.19:194-203.

Wu X, Wu T, Long J, Yin Q, Zhang Y, Chen L, Liang Y, Liu R, Gao T and Dong H (2007) Productivity and biochemical properties of green tea in response to a bacterial type-III effector protein and its variants. J Bioscience 32:1119–1132.

Yoshida J, Kobayashi T (1999) Intracellular hyperthermia for cancerusing magnetite cationic liposomes. J Magn Mater 194:176-184.

Zheng L, Hong F, Lu S, Liu C (2005) Effect of nano-TiO_2 on strength of naturally aged seeds and growth of spinach. Biological Trace Element Research 104:83-91.

----------********----------